Universitat d'Alacant
Universidad de Alicante

Materiales espumados metálicos con inclusiones térmicas de base carbono y nanoingeniería interfacial

Lucila Paola Maiorano Lauria

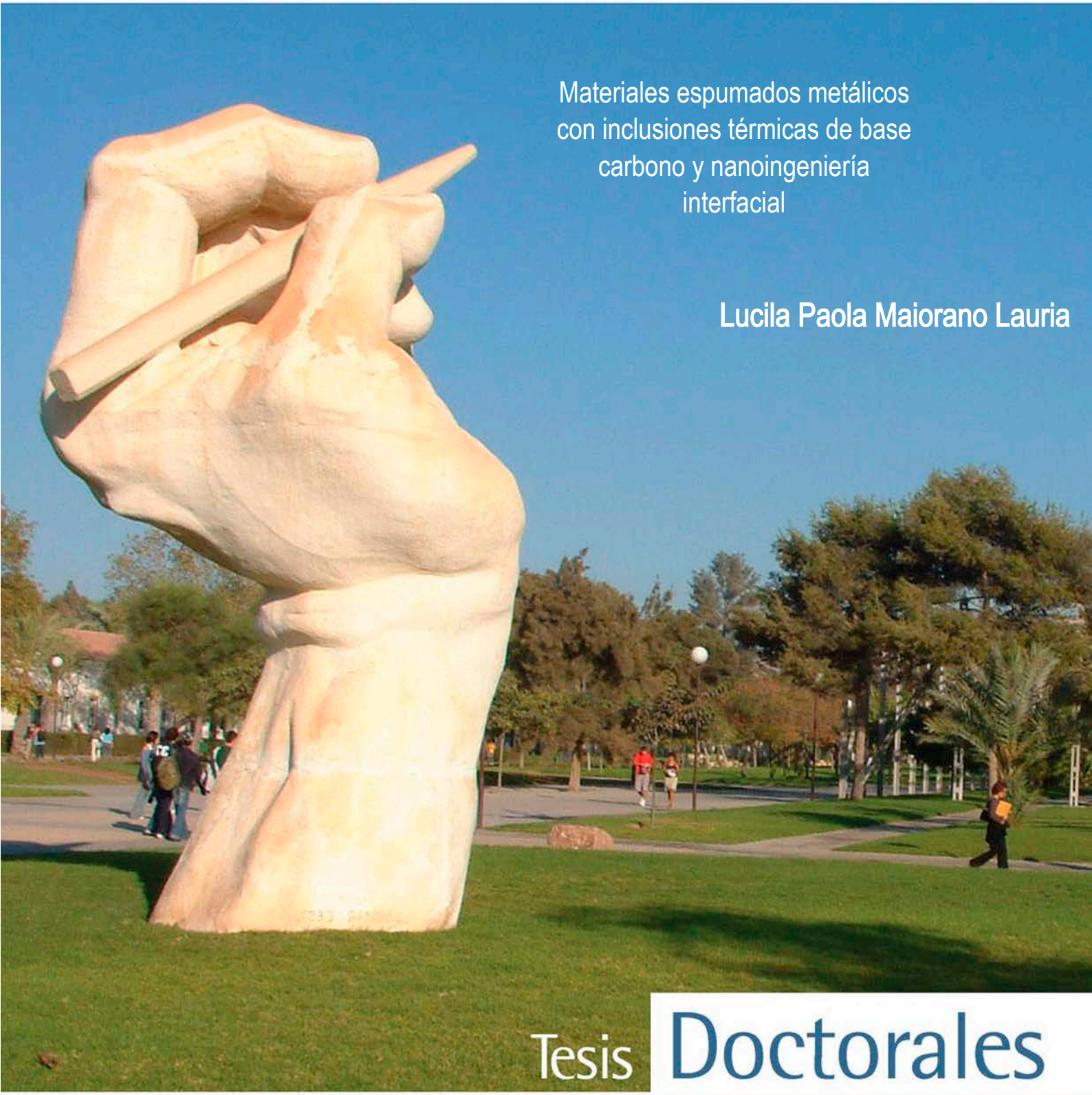

Tesis Doctorales

UNIVERSIDAD de ALICANTE

Unitat de Digitalització UA
Unidad de Digitalización UA

DEPARTAMENTO DE QUÍMICA INORGÁNICA

INSTITUTO UNIVERSITARIO DE MATERIALES DE ALICANTE

FACULTAD DE CIENCIAS

MATERIALES ESPUMADOS METÁLICOS CON INCLUSIONES TÉRMICAS DE BASE CARBONO Y NANOINGENIERÍA INTERFACIAL

LUCILA PAOLA MAIORANO LAURIA

Tesis presentada para aspirar al grado de

DOCTOR/DOCTORA POR LA UNIVERSIDAD DE ALICANTE

MENCIÓN DE DOCTOR/DOCTORA INTERNACIONAL

DOCTORADO EN CIENCIA DE MATERIALES

Dirigida por:

Prof. Dr. JOSÉ MIGUEL MOLINA JORDÁ

Tesis Doctoral financiada por el Ministerio de Ciencia e Innovación a través del proyecto MAT2016-77742-C2-2-P y por el Vicerrectorado de Investigación y Transferencia de Conocimiento de la Universidad de Alicante, mediante las ayudas destinadas a la formación predoctoral 2018 (UAFPU2019-33)

Universitat d'Alacant
Universidad de Alicante

D. José Miguel Molina Jordá, Prof. Titular del Departamento de Química Inorgánica de la Universidad de Alicante,

CERTIFICA QUE:

El presente trabajo titulado "MATERIALES ESPUMADOS METÁLICOS CON INCLUSIONES TÉRMICAS DE BASE CARBONO Y NANOINGENIERÍA INTERFACIAL" ha sido realizado en las dependencias del Instituto Universitario de Materiales de Alicante y del Departamento de Química Inorgánica de la Universidad de Alicante por la licenciada en química Lucila Paola Maiorano Lauria bajo mi dirección y autorizo su presentación para optar al grado de Doctor/a con mención internacional en Ciencia de Materiales.

Y para que conste a los efectos oportunos, firmo la presente certificación en Alicante, a _____ de _____ de 2022.

Fdo. Dr. José Miguel Molina Jordá
Profesor Titular
Departamento de Química Inorgánica

To my family.
to my new family,

for your endless support.

Acknowledgements/ Agradecimientos

Es curioso cómo experimentamos día a día todas esas expresiones que a menudo difundimos. "*La vida da mil vueltas*", decimos constantemente. Y acompañada a esa expresión, se desarrollaron mis últimos años. En un entramado de situaciones, coincidencias, o quizá, porque "*fue cosa del destino*", mi camino giró en alguna esquina para terminar donde hoy estoy, con una carrera en investigación que nunca pensé fuera a ser para mí. Un recorrido lleno de esfuerzos, logros y satisfacción que realicé acompañada de mucha gente que merece, entre muchas cosas, mis agradecimientos.

A mi director y tutor de tesis, compañero y amigo, José Miguel. Este trabajo no habría sido posible sin tu incondicional apoyo. Gracias por haber puesto tu confianza en mí, por contagiarme tu pasión por lo que hacemos, por tus infinitas horas de dedicación y tu absoluta disponibilidad. Ahí estás, mañanas, tardes y noches, para ayudarme a seguir avanzando. Sin duda, tu fuerza de voluntad es admirable. Gracias por haberme recordado cada día que "*todo esfuerzo tiene su recompensa*" y, pese a que en ocasiones no me gusta darte la razón, en esto seguro la tenías. "*Empecé desde abajo*" y a base de trabajar juntos "*codo con codo*" conseguí hasta una beca que, como poco, me (nos) llenó de orgullo y alegría.

Todo lo que sé, lo sé gracias a ti.

Quiero agradecer al Vicerrectorado de Investigación de la Universidad de Alicante por haberme otorgado un contrato de formación pre-doctoral y una ayuda adicional para realizar una estancia de tres meses en el extranjero. Sin duda, esta financiación permitió que pudiera llevar los desarrollos de esta tesis un poco más lejos. Así mismo, siento una enorme gratitud por todo el personal (tanto administrativo como docente e investigador) del Departamento de Física Aplicada. Gracias por haber compartido vuestro espacio de trabajo conmigo (con nosotros) durante todos estos años y por haberme hecho "*sentir como en casa*".

Este camino no habría sido tan grato si no lo hubiera recorrido de la mano de increíbles compañeros de grupo. To my longest-term colleague Cagla, thank you for always bringing a friendly smile to the lab and lightening the difficult moments. A mis compañeros jóvenes, "*ahí va una*" para vosotros. A Natalia, Ramón, Alejandro, Maroua y Mokhtaria, gracias por haber depositado vuestra

confianza en mí, por haberme hecho "*sentir grande cuando me sentía pequeñita*" y, en ocasiones, muy mayor de edad. A Noe, sí, tu también eres joven. Gracias infinitas por todo lo anterior y por ser una gran compañera, confidente y amiga. Me llevo conmigo cada momento en el que escuchabas en el lab mis explicaciones "*con ojos y oídos puestos*", con entusiasmo. Gracias, chicos, he aprendido mucho de vosotros. Me habéis ayudado a crecer.
Cris, mi compañera de viaje desde nuestra iniciación en la química, "*¿quién nos lo iba a decir?*". Pues sí, aquí estamos, más de 15 años después compartiendo el desayuno de cada mañana. Gracias, amiga por ser mi "*vía de escape*", por ser un ejemplo a seguir. Deseo de todo corazón que en los próximos 15 años sigamos bajando a por ese rápido café anti-estrés.

I would like to express my gratitude to Professor Oronzio Manca for opening me his lab in Italy and giving me the opportunity to work with his research group. I would also like to acknowledge Professor Bernardo Buonomo for his patience and the time he spent teaching me very kindly. Renato, my pc partner, thanks for making my stay so comfortable. I acknowledge you, Silvio, for your absolute availability and your excellent way of driving, and also you, Sergio, for your openness to work together. Grazie mille!

Y cómo iban a faltar mis amigos. Todos y cada uno de ellos, que han vivido día a día "*mis alegrías y mis penas*". A Tania, Salva, Esther, Luis y David, gracias por escucharme, animarme, ayudarme, por estar siempre, siempre, siempre ahí. Gracias por "*tirarme de las orejas*" cuando me lo merecía y por acompañarme en mis logros y hacerlos también vuestros. A mis amigas "*de toda la vida*" Patri, Mire y Eli, gracias por seguir estando ahí, aunque en estos últimos años…yo haya estado haciendo una tesis.

Todavía recuerdo el día que le planteé a mi familia la posibilidad de hacer una tesis. Allí estábamos, comiendo juntos en un restaurante frente a casa, donde prometí que esta nueva aventura me llevaría no más de 3 años. Pero, como siempre en esta vida, "*mi camino dio mil vueltas*". Tardé un poco más, pero llegué a la recta final con más fuerza. Gracias por haberme escuchado y animado aquel día en el restaurante a hacer esta tesis. De no haber sido así, no habría conseguido lo que hoy en día más me enorgullece. Mamá, papá, Franquito, gracias por todo el apoyo que me dais "*en las buenas y en las malas*". ¡Os quiero!

Y por último, Jero, mi compañero de vida… estaré eternamente agradecida por tu apoyo. Gracias por ir conmigo de la mano durante estos años tan locos, tan duros, por empujarme a seguir adelante cada vez que quise "*tirar la toalla*", por ponerle luz con tu alegría a mis muchos días grises, por hacer que todo sea fácil, sencillo. Gracias por creer en mi. ¡Te quiero!

List of contents

Abstract

The present PhD Thesis is framed in the field of Materials Science, particularly in the development of metal foams with interconnected porosity (also known as open-pore foams) for heat dissipation applications. This development concerns the predesign of the materials, their manufacture and subsequent microstructural, thermal, fluid-dynamic and mechanical characterisation.

Open-pore metal foams exhibit high specific surface area per unit volume, low density, high heat transfer capacity, as well as acceptable mechanical properties. The combination of these properties together with an interconnected porous structure which allows the passage of a fluid through it, makes these materials excellent candidates for numerous applications in the field of electrochemistry as electrodes, in catalysis as catalytic supports, in biomedical engineering where they are used as biocompatible and biodegradable implants and in the electronics area as heat sinks and heat exchangers.

In recent years, thermal management in electronics, aeronautics and aerospace industries has become a focus of study for many authors because of current technological advances, which imply a miniaturisation of electronic devices and an increase in their power and performance. Under normal operating conditions, the most modern devices generate large amounts of heat that must be removed to avoid failure and breakage of the electronic packaging. In its simplest form, the architecture of these electronic packages consists of a silicon chip (the heat emitter) followed by a ceramic material that acts as an electrical insulator (usually of AlN) and two types of materials responsible for removing the heat excess. On the one hand, there are the well-known passive heat sinks, characterised by their high thermal conductivity and low thermal expansion coefficient. These components conduct the heat through their structure to further zones where an active heat sink is located. Metal/ceramic composites, such as aluminium/diamond and aluminium/graphite, are good examples of passive heat sinks. Numerous authors reported that the performance of these materials can be improved by nano-engineering the matrix-reinforcement interface, resulting in composites with superior thermal conductivity, low thermal expansion coefficients and, in some cases, improved mechanical properties. Active heat sinks, on the other hand, transport heat by conduction through the solid structure of the material and then transfer it by convection to a moving fluid through its internal structure, which removes the heat to the medium. The most common active heat sinks are the well-known aluminium fin heat sinks. These are sometimes replaced by open-pore metal foams as they exhibit higher specific surface area, greater heat transfer coefficient, as well as good thermal conductivity and reduced density. Figure 1 provides a simplified illustration of the architecture of an electronic packaging in which an aluminium fin active heat sink is employed (Figure 1a) and one in which the active heat sink is replaced by an aluminium foam (Figure 1b). Also, the heat transfer mechanisms occurring during the operation of these packages are depicted in Figure 1c and 1d.

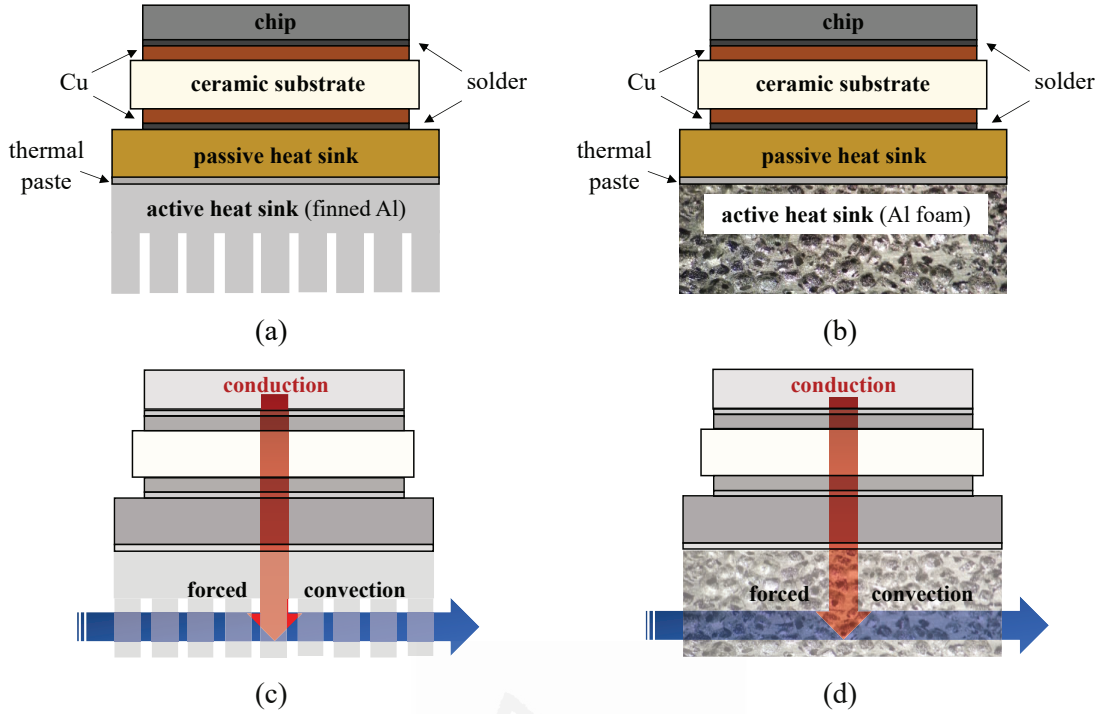

Figure 1. Electronic packaging architecture (a,b) and heat transfer mechanisms occurring under operating conditions (c,d) when using different active heat sinks: aluminium fins (a,c) or aluminium foam (b,d).

There are two strategies for generating porosity in open-pore foams: i) self-formation, where porosity is generated through a process of evolution according to physical principles, and ii) predesign, where the structure is created in a more controlled manner using martyr moulds that determine the pore cavities. The manufacturing techniques of open-pore foams in which porosity generation is controlled using a predesign strategy can be classified into four groups according to the state of the precursor material: liquid, solid, vapour and ions. When the precursor material is in a liquid state, the most important processing methods are investment casting of polymeric foams and casting around space holders or infiltration on martyr preforms. If the processing is carried out with a solid-state precursor, techniques such as partial sintering of powders and fibres, pressurisation and sintering of powders in martyr preforms, sintering of hollow spheres, sintering of powders and binders or reaction of multicomponent systems can be highlighted. Likewise, the processing of foams in the vapour and ionic state concerns the vapour deposition and electrodeposition, respectively, of the precursor material on polymeric foams.

Among the wide variety of manufacturing techniques, the infiltration of martyr preforms, also known as replication method, appears to be the most interesting as it allows the best control over the material. This method has traditionally been used to obtain open-pore metal foams. The replication method, shown in Figure 2, consists of producing a porous preform, usually of packed particles, with a templating agent (sodium chloride, carbon, etc.) which is then infiltrated with

molten metal or any other matrix liquid precursor to produce a composite material. After solidification of the liquid precursor, the preform is removed either by dissolution or by controlled chemical reaction (for e.g., combustion) to leave an interconnected porous structure which can be considered as the "negative" of the initial preform.

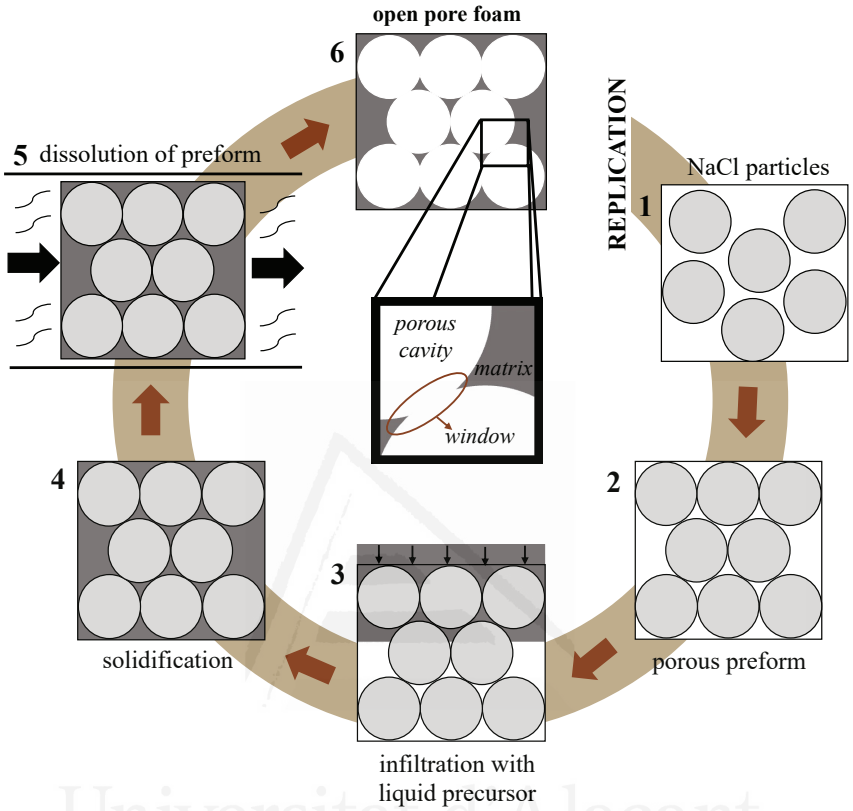

Figure 2. Replication method processing steps for open-pore foams using NaCl martyr particles as template agent.

This method has the advantage of being sufficiently versatile to allow control of volume fraction, size, shape and pore size distribution. With this precise control, the properties of the manufactured foams can be easily adjusted to a desired range. Depending on the precursor material and the desired final pore architecture, different raw materials have been employed to prepare martyr preforms. However, the most commonly used material is sodium chloride (NaCl) in particulate form, which can be conveniently packed and infiltrated with liquid precursors at temperatures below its melting point (801°C) and then removed by dissolution in aqueous solutions. Metal foams obtained by the replication method are characterised by their low porosity (less than 70%), resulting in materials with higher pressure drops than commercial metal foams, but with a clear advantage over the latter: the ability to dissipate large amounts of heat flow because of a high metal volume fraction.

A literature review over the last few years reveals that several authors have adopted the strategy of incorporating new phases into open-pore foams, as it seems to be a suitable way to overcome the

requirements of many applications such as structural, catalytic, electrochemical and biomedical. However, there are few precedents where such strategy is considered for modifying materials applied to active thermal management. Despite the great attributes of traditional metal foams used for heat dissipation, the accelerated technological growth makes their performance insufficient to meet the requirements of the most advanced electronic devices. Therefore, it is necessary to reformulate their designs in order to enhance their properties.

The development of this PhD Thesis arises in view of these ongoing problems, the hypotheses of which are set out below:

1. Metal foams, extensively used for thermal dissipation, exhibit properties that have limited their use in emerging technologies, so their designs need to be reformulated. The strategy of incorporating new phases into the structural matrix of metal foams seems to be the most appropriate way to extend their applicability.
2. The replication method, commonly used for the manufacture of open-pore metal foams, is sufficiently versatile to allow control over the porous structure of the final material. The use of martyr preforms for the generation of porosity from a templating agent makes the incorporation of new phases into the packaging entirely feasible, as long as certain design aspects must be taken into consideration. Examples of these are, among others, that the incorporated phases should not break the coordination of the templating agent particles in such a way that they are unable to be removed after infiltration, and thus prevent interconnection between pores in the final material; or that the matrix-inclusion system should present a poor thermal and/or mechanical interface.
3. The use of carbon-based reinforcements in aluminium matrix composites, such as graphite flakes or diamond, have provided thermal conductivities much higher than that of analogous monolithic materials, and can therefore be considered as potential thermal inclusions in open-pore metal foams.
4. Since heat removal in active heat sinks occurs by a conduction/forced convection mechanism, materials with higher thermal conductivity will be able to conduct heat more effectively to further zones from the heat emitter, that will then be transported by a fluid and removed to the medium. Therefore, open-pore metal foams with carbon-based thermal inclusions are expected to provide higher power dissipation compared to traditional metal foams.

Based on these hypotheses, the following general objectives are formulated:

1. Development of open-pore aluminium foams containing graphite flakes as thermal inclusions (aluminium/graphite flakes composite foams) and evaluation of their applicability in the field of active heat dissipation.

2. Development of open-pore aluminium foams containing diamond particles as thermal inclusions (aluminium/diamond composite foams) and evaluation of their applicability in the field of active heat dissipation.
3. Use of interfacial nano-engineering to modify the properties of open-pore aluminium foams with carbon-based thermal inclusions (graphite flakes and diamond particles) and evaluation of their applicability in the field of active heat dissipation.

In addition, the specific objectives are listed below:

1. Design and fabrication of open-pore aluminium foams incorporating graphite flakes, using the replication method and varying the volume fraction of the present phases.
2. Design and fabrication of open-pore aluminium foams incorporating diamond particles, using the replication method and varying the volume fraction of the present phases.
3. Design and fabrication of aluminium/graphite and aluminium/diamond composite foams with modified metal-inclusion interfaces, using the replication method and the interfacial nano-engineering.
4. Microstructural characterisation of the fabricated materials, in which the orientation of the graphite flakes, the distribution of the inclusions in the matrix phase, the morphology and pore connecting window sizes, as well as the generated metal-inclusion interfaces will be evaluated.
5. Fluid-dynamic characterisation of the manufactured materials, evaluating their pressure drop and permeability.
6. Thermal characterisation of the manufactured materials, considering properties such as thermal conductivity and power dissipation under operating conditions.
7. Mechanical behaviour evaluation of the manufactured materials by means of three-point bending tests.
8. Use of computational simulation tools for thermal modelling of aluminium/diamond composite foams and verification of the experimental results.
9. Assessment of viability of the manufactured materials for their use as heat sinks in active thermal management applications.

The fulfilment of the stated objectives is evidenced by the development of the following four chapters. Two of them were published as scientific articles in journals indexed in Journal Citation Reports - JCR (Chapter 1 and 3 in the first quartile), another was published as an open access book chapter (Chapter 2) and the last one is in the process of being published as a scientific article in a first decile journal (Chapter 4). The achievement of all of them constitutes a thematic unit of high scientific-technological interest, providing a new range of applicability for open-pore foams in terms of active thermal management. It is also believed that the development of the materials here

presented, as well as the techniques used for their fabrication, can be a new exploratory path for their application not only in the electronics industry, but also in others such as biomedical and catalytic.

Chapter 1. Challenging thermal management by incorporation of graphite into aluminium foams

Chapter 1 of this PhD Thesis proposes the design, fabrication and characterisation of a new family of open-pore aluminium foams with graphite flakes as thermal inclusions. The new materials were inspired by the union of two ideas: the use of carbon-based inclusions as thermal conductivity enhancers and the exploitation of the fluid-dynamic advantages provided by materials with an interconnected porous structure. The advantages of graphite flakes (Gf) as thermal inclusions include low density, easy machining and high anisotropy. The latter has an impact on properties such as thermal conductivity (1000-2000 $Wm^{-1}K^{-1}$ in the basal plane and 38 $Wm^{-1}K^{-1}$ in the perpendicular plane), thermal expansion coefficient (-1×10^{-6} K^{-1} in-plane, 28×10^{-6} K^{-1} out-of-plane) and mechanical behaviour.

Composite foams were fabricated by the well-known replication method. For this purpose, porous preforms consisting of packed sodium chloride and oriented graphite flakes conveniently distributed were prepared. The preforms were infiltrated by gas pressure with liquid aluminium, which was rapidly solidified to avoid the formation of reaction products at the metal-inclusion interface. The NaCl particles were then removed by dissolution, resulting in two families of materials differing in the distribution of inclusions in the matrix phase: i) aluminium foams with homogeneously distributed oriented graphite flakes in the matrix and ii) materials consisting of alternating layers of aluminium foam and oriented graphite flakes. Both structures are shown in Figure 3.

The preparation of porous preforms, which commonly consist of single nature, size and morphology particles packings, was found to be a critical step in the development of these materials due to the incorporation of a new phase. In order to optimise the system, a comprehensive study on preforms packing was carried out, involving the use of different compaction pressures, as well as varying the volume fractions of the present phases (NaCl, Gf and pore). The results revealed that those preforms prepared from homogeneous mixtures of NaCl and oriented Gf had two clear restrictions. The first one is determined by the coordination of the NaCl particles, which must guarantee an efficient and complete dissolution process of the templating agent and can be understood as a percolation limit. The NaCl particles had to form an interconnected network with a coordination number for each particle of at least 3. Consequently, and considering results from other published works, the NaCl volume fractions were limited to a minimum value of 0.3. The other restriction entails the

impossibility of manufacturing samples with specific compositions as a consequence of gravity packing and was defined as the compaction limit. This restriction prevents the preparation of preforms having high porosity (pore volume fractions greater than 0.45) and low Gf content (Gf volume fractions smaller than 0.30). In the case of preforms in which the graphite flakes are found forming alternating layers with the NaCl packings, no percolation restriction is applicable. In an extreme case where the volume fraction of NaCl is so small compared to that of Gf that generates layers of the NaCl particle thickness, the coordination of these is still sufficient to be effectively removed. In contrast, the minimum compaction limit was also detected in this system for preforms prepared without external pressure because of the natural tendency of the NaCl and graphite flake particles to settle one on top of each other.

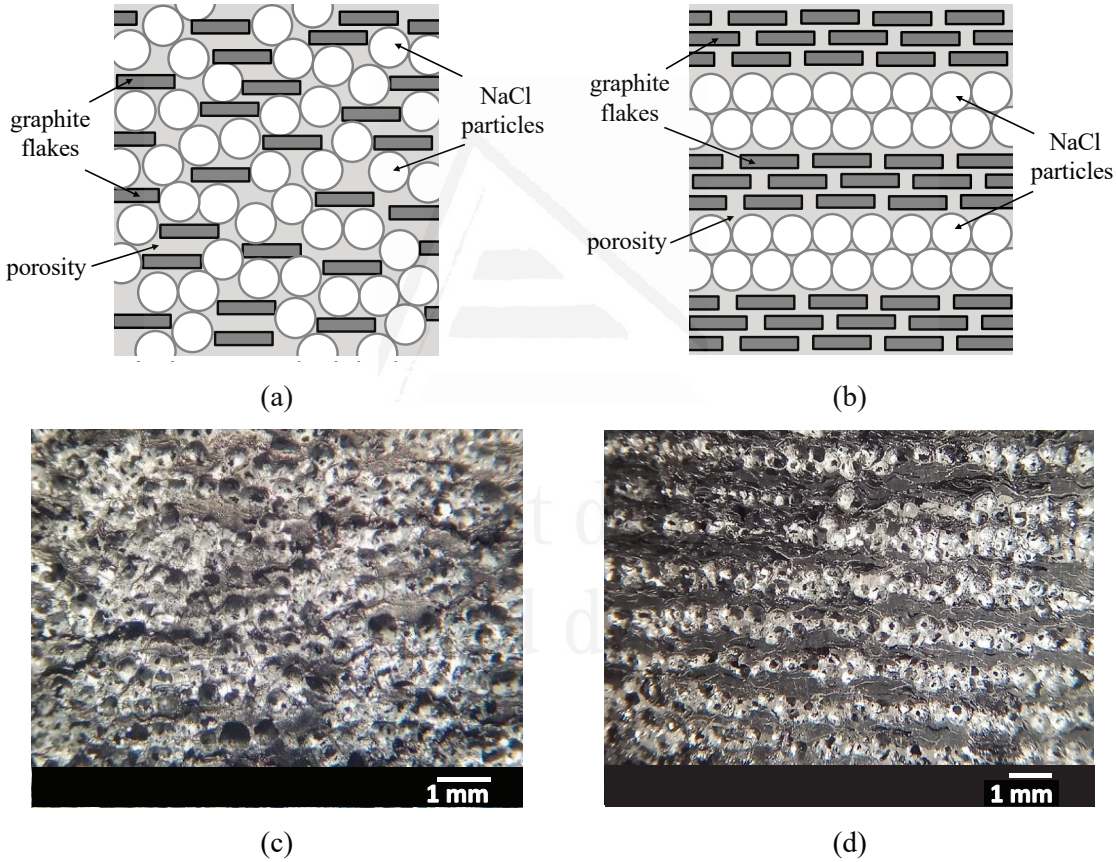

Figure 3. Schematic representation of the preforms structures (a,b) and optical images of the fabricated foams (c,d). (a,c) refer to aluminium foams with oriented graphite flakes homogeneously distributed in the matrix, while (b,d) refer to materials consisting of alternating layers of aluminium foam and oriented graphite flakes.

The systems optimisation allowed the fabrication of a set of materials which were subsequently characterised. Foam permeabilities were obtained by experimental methods and verified by means of an analytical model. The application of the model, supported by a microstructural study to

establish the pore connecting window size distribution in the foams, determined that the calculated permeability values were in better agreement with the experimental results when the pore connecting windows considered were the smallest ones. As expected, foams presented lower permeabilities as their porosity decreased. Since the incorporation of graphite flakes in the aluminium foams leads to a decrease in the overall porosity of the materials, they generated higher pressure drops at forced air flow than the aluminium foams, but with values still suitable for the most demanding thermal management applications in the electronics industry.

The thermal behaviour of the new materials was also evaluated through experimental measurements of thermal conductivity and power dissipation under operating conditions using devices designed and assembled in the laboratories of the University of Alicante. The composite foams provided excellent longitudinal thermal conductivities (being the graphite flakes aligned with the heat flow), within the range of 60-290 $Wm^{-1}K^{-1}$. These values were predicted by known theoretical models considering the two characteristic microstructures of both types of fabricated materials. On the other hand, the composite foams registered power dissipations up to 325% higher than that of conventional aluminium foams also manufactured by the replication method.

In addition to the thermal performance, it is of great interest to know the mechanical response of these materials as they are usually assembled in electronic modules by means of anchors that impose a certain bending stress. For this purpose, foams were subjected to 3-point bending tests on a universal testing machine. It is well known that graphite flakes are mechanically inefficient when used as reinforcement in metal matrix composites, a feature that was transferred to the foams fabricated here. When graphite flakes were incorporated into the porous structure, the flexural moduli were found to be slightly lower than that of aluminium foams, but much superior to other foam materials used for active thermal management, making these materials excellent candidates for their use as heat sinks.

Chapter 2. Open-pore foams modified by incorporation of new phases: multiphase foams for thermal, catalytic and medical emerging applications

The incorporation of new phases in the structural matrix of open-pore foams has proved to be a strategy used by several authors to adjust the properties of these materials according to the desired application. However, until the development of this chapter, there were no works in the literature that reflected the necessity of redesigning these materials or compiled the different strategies used to obtain them. The content of Chapter 2 deals with the various manufacturing techniques, both for conventional open-pore foams and for those incorporating new phases (here referred to as multiphase open-pore foams).

Developed multiphase open-pore foams are still scarce and can be manufactured by two distinct methods depending on the desired final structure. On the one hand, the incorporation of new phases in monolithic materials is achieved by preloading particles (inclusions) into the porous preform, by preloading particles into the matrix precursor liquid, or by electrodeposition. This results in composite foams or foams with host phases in the porous cavities of the material, both with a homogeneous dispersion of the new phases in a continuous matrix. The second method used to obtain multiphase foams is based on combinations of monolithic materials, usually characterised by an alternating layered structure. These include fin foams, which are obtained by joining pre-existing porous and non-porous monoliths (discontinuous matrix) or by casting a precursor liquid in a mould with pre-existing and conveniently located martyr preforms (continuous matrix). In both cases, the non-porous material is considered the new phase. The mould may also contain martyr preforms alternated with packed particles (inclusions), resulting in composite fin foams with a continuous matrix.

Finally, the chapter reviews the development of some materials using the methods described above, designed for thermal, catalytic and medical applications.

Chapter 3. Guiding heat in active thermal management: One-pot incorporation of interfacial nano-engineered aluminium/diamond composites into aluminium foams

Given the excellent performance of the materials developed in Chapter 1 for active heat dissipation, it was considered the necessity to explore new composite foams incorporating other carbon-based thermal inclusions. It is well known that diamond particles are widely selected as reinforcement in aluminium matrix composites for their use as passive heat sinks in thermal management applications. These materials have low thermal expansion coefficients and high thermal conductivities which, in addition, can be conveniently adjusted by controlling the reaction at the aluminium-diamond interface during processing. This chapter discusses the design, fabrication and subsequent characterisation of foam materials that combine the passive dissipation properties of aluminium/diamond composites with the high active dissipation capacity of aluminium foams.

The new materials, fabricated by the replication method, required the preparation of porous preforms consisting of alternated layered packings of NaCl (martyr particles) and diamond particles (Figure 4a). The gas pressure-assisted infiltration process of the porous preforms with liquid aluminium was carefully controlled to nano-engineer the reaction products at the aluminium-diamond interface. For this purpose, the time from the point at which the maximum pressure is reached in the infiltration chamber was varied. During this time (here called contact time), the liquid metal remains in contact with the diamond particles, determining the reactivity of the system and thus the quality of the interface generated. In the present study, contact times of 0, 15 and 45 minutes

were selected. After these times, the metal was solidified and the NaCl particles were removed by dissolution. As a result, multicomponent materials structured in alternating layers of aluminium foam components and aluminium/diamond composite components were obtained. The optical image in Figure 4b shows their representative structure. The different sets of materials produced presented a longitudinal or transverse arrangement of the alternating layers of each component, as well as different composite:foam volume ratios (27:73, 35:65 and 70:30).

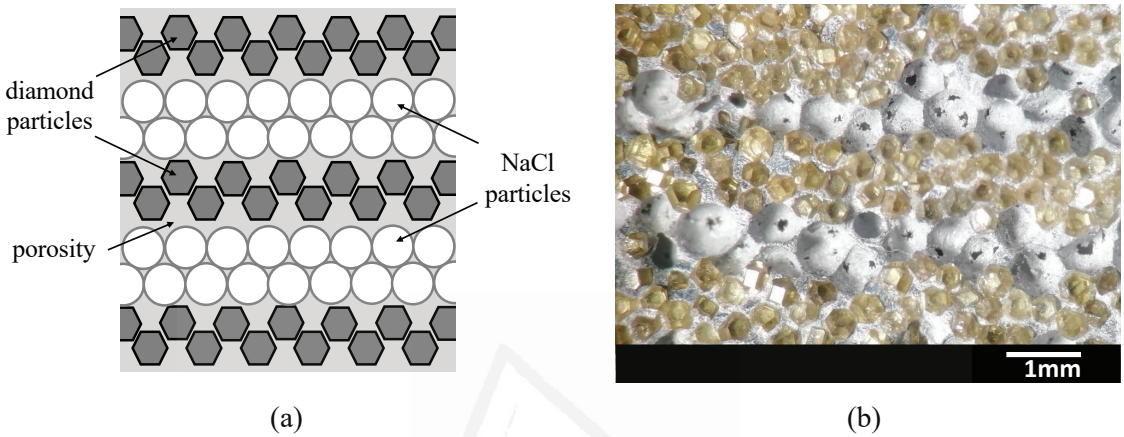

Figure 4. Representation of a packed preform consisting of alternating layers of NaCl and diamond particles (a) and optical image of a multicomponent material resulting from the infiltration of a preform like (a) with liquid aluminium.

Like foams incorporating graphite flakes, the preparation of the new materials presents certain restrictions associated with the packing of particles into the preforms. As noted in Chapter 1, NaCl and Gf particles can be compacted in alternating layers with an external pressure to produce self-standing preforms due to the flexibility of the graphite flakes and the local deformations that the NaCl particles can suffer. This technique allows obtaining preforms with a wide variety of volume fractions of each phase. However, it is not possible to generate self-standing preforms using NaCl and diamond particles by applying external pressure due to the diamond's characteristic of being non-deformable. These preforms can only be produced in a narrow band delimited by the upper and lower limits of the packing volume fractions of NaCl particles (within the 0.58-0.63 range) and of diamond particles (within the 0.60-0.61 range). In these intervals, the lower values correspond to the minimum compaction achieved by the natural arrangement of the particles when they are subjected to vibrations. The upper values correspond to the compaction value when particles are carefully packed with the help of a manual piston, allowing a “better” accommodation of particles. The microstructural characterisation of the multicomponent materials was carried out using optical microscopy and scanning electron microscopy (SEM) allowing the observation, respectively, of the overall materials structure and reaction products (Al_4C_3 crystals) at the aluminium-diamond interface.

The thermal behaviour of the manufactured materials was evaluated by means of thermal conductivity and power dissipation measurements, using devices designed and assembled at the University of Alicante. The results indicated that the processing conditions affect the thermal performance of the materials, with those manufactured at contact times of 15 minutes providing the highest thermal conductivity. Thermal conductivity values reached 435 $Wm^{-1}K^{-1}$ when the multicomponent material had a longitudinal arrangement (the arrangement of the alternating layers was parallel to the heat flow) and a composite:foam component volume ratio of 70:30. In addition, this material provided power dissipation under working conditions up to 130% higher than that of conventional aluminium foams manufactured by the replication method. The thermal conductivity values were discussed using well-known analytical models that consider a system of alternating semi-infinite layers of composite material and metal foam, while the power dissipations were corroborated by finite element modelling using the computational simulation tool Ansys-Fuent.

Furthermore, the materials were mechanically characterised by means of 3-point bending tests with a universal testing machine. The mechanical properties of the multicomponent materials were found to scale with thermal conductivity, indicating that the generation of an optimal thermal interface leads to the best mechanical metal-particle interface in the composite components. The flexural modulus value for the thermally optimised material was found to be half than that of an aluminium/diamond composite material obtained under the same processing conditions and almost 20 times higher than that of conventional aluminium foams. Since these do not pose flexural failure problems when integrated into electronic packagings, it can be concluded that the multicomponent materials developed in this study exceed the minimum mechanical requirements of these applications.

Results suggest that the presence of high thermal conductivity aluminium/diamond composite components can significantly improve the heat dissipation of conventional aluminium foams, as they mainly act as effective thermal guides that conduct heat and transfer it to the aluminium foam components where dissipation is achieved by forced convection. The high heat transfer between layers, caused by the presence of a continuous metal matrix between the two components, makes these materials serious candidates for active thermal management applications.

Chapter 4. Al/Gf composite foams with SiC-engineered interfaces for the next generation of active heat dissipation materials

The results derived from the studies carried out in Chapter 1 and 3 inspired the development of the present chapter. The latter focuses on the modification of aluminium/graphite composite foams by the incorporation of silicon carbide at the metal-inclusion interface in order to improve their thermal and mechanical properties.

Literature reports numerous studies in which graphite flakes are used as reinforcement of composite materials to be used as passive heat sinks. However, the excellent properties of graphite flakes are often not transferred to the final composite materials due to the weak interfacial bonding between aluminium and graphite flakes, which is mainly due to poor wetting of the matrix-reinforcement system. It has been shown that interfacial engineering can improve the thermal and mechanical properties of these materials by coating the graphite flakes with ceramic phases such as metal carbides. This idea was applied in the present chapter to the development of improved aluminium/graphite flake composite foams.

The new materials were fabricated by the replication method. For this purpose, two sets of porous preforms differing in particle average size were prepared: i) 105 μm NaCl preforms containing a homogeneous distribution of 150 μm Gf oriented and coated with SiC and ii) 305 μm NaCl preforms containing a homogeneous distribution of 500 μm Gf oriented and coated with SiC. The preforms were then gas pressure infiltrated with liquid aluminium using zero contact time. After the metal solidification, the templating agent was removed by dissolution, resulting in composite foams with an interconnected porous structure. The optimisation of the interface and, therefore, of the materials performance, was carried out using Gf with different degrees of SiC coating. For this purpose, the well-known molten salt synthesis method was used, and the treatment time was varied from 1 to 60 minutes. Figure 5 details the structure of a preform prepared for its infiltration with liquid aluminium, as well as the interdiffusion process occurring at the Gf-silicon interface during the graphite flakes coating.

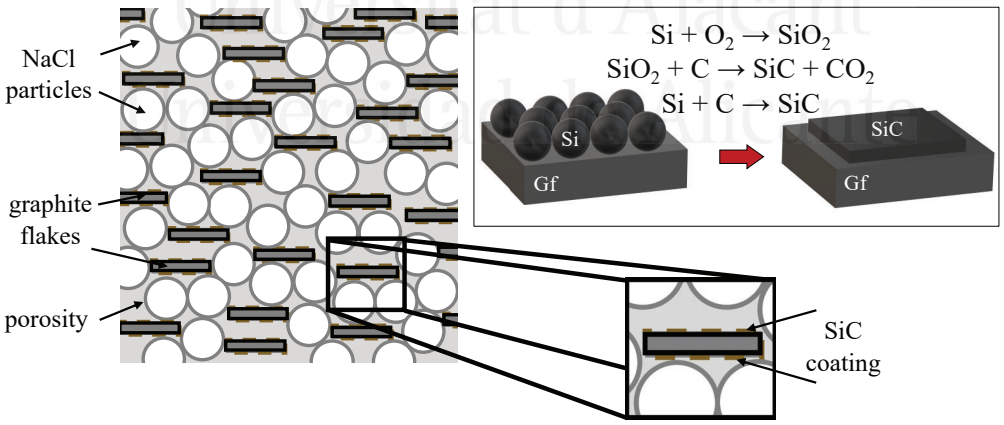

Figure 5. Representation of a NaCl preform containing SiC-coated graphite flakes oriented and homogeneously distributed and interdiffusion process occurring at the interface between Gf and silicon particles during the Gf coating with molten salts.

The morphology and chemical composition of the graphite flake coatings were analysed using various characterisation techniques such as scanning electron microscopy (SEM), SEM-coupled X-ray spectroscopy (SEM-EDX) and X-ray diffraction (XRD). The results confirmed that the coatings

generated on the graphite flakes by the molten salt synthesis method were of SiC and showed discontinuity, even in those cases where longer treatment times were employed.

Pressure drop measurements indicated that composite foams with larger pore sizes (derived from the use of large NaCl particles) resulted in higher permeabilities. As in Chapter 1, an analytical model was used to predict the fluid-dynamic behaviour of the materials. This model, supported by a microstructural analysis which allowed the determination of the pore connecting window size distribution, again established that the calculated permeabilities better correlate with the experimental measurements when the smallest average window sizes were considered.

The thermal performance of the foam materials was also evaluated by means of experimental measurements of thermal conductivity and power dissipation under operating conditions. For this purpose, devices designed and assembled in the laboratories of the University of Alicante were used. The best thermal conductivity recorded was 232 $Wm^{-1}K^{-1}$ for the foam containing 500 μm Gf coated during a 10-minute treatment and a longitudinal arrangement (with the Gf oriented parallel to the heat flow). The heat dissipation of the optimised material was also found to be approximately 500% higher than that of conventional aluminium foams and 104% higher than that of aluminium/graphite foams with unmodified interfaces.

On the other hand, mechanical characterisation was carried out by subjecting the materials to 3-point bending tests with a universal testing machine. Like the multicomponent material presented in Chapter 3, the composite foams with a Gf of 500 μm and the best thermal interface were found to have the best mechanical behaviour of its group. The flexural modulus was found to be twice that of an analogous foam with unmodified interface. In their entirety, the results suggest that this foam material can be considered an excellent candidate for future generations of active heat sinks in electronics.

Resumen

La presente Tesis Doctoral se enmarca en el campo de la Ciencia de Materiales, en concreto, en el desarrollo de materiales espumados metálicos con porosidad interconectada (también conocidos como espumas de poro abierto) para aplicaciones de disipación térmica. Dicho desarrollo concierne el prediseño de los materiales, su fabricación y una posterior caracterización microestructural, térmica, fluidodinámica y mecánica.

Las espumas metálicas de poro abierto presentan elevada superficie específica por unidad de volumen, baja densidad, gran capacidad de transferencia de calor, así como unas propiedades mecánicas aceptables. La combinación de estas propiedades junto con una estructura porosa interconectada que permite el paso de un fluido a su través hace de estos materiales excelentes candidatos para numerosas aplicaciones en el campo de la electroquímica como electrodos, en catálisis como soportes catalíticos, en ingeniería biomédica donde se utilizan como implantes biocompatibles y biodegradables y en el área de la electrónica como disipadores e intercambiadores de calor.

En los últimos años, el control térmico en la industria electrónica, aeronáutica y aeroespacial se ha convertido en un foco de estudio de numerosos autores como consecuencia de los grandes avances tecnológicos actuales, que implican una miniaturización de los equipos electrónicos y un aumento de la potencia y prestaciones de los mismos. En condiciones normales de operación, los equipos más modernos generan grandes excesos de calor que deben ser eliminados con el fin de evitar fallos y roturas de los empaquetados electrónicos. La arquitectura de estos empaquetados electrónicos, en su forma más simple, consiste en un chip de silicio (foco emisor de calor) seguido de un material cerámico que cumple la función de aislante eléctrico (normalmente, de AlN) y de dos tipos de materiales responsables de eliminar los excesos de calor. Por un lado, se emplean los conocidos disipadores pasivos, caracterizados por presentar elevada conductividad térmica y bajo coeficiente térmico de expansión. Estos componentes conducen el calor a través de su estructura hasta zonas más alejadas donde se localiza un disipador activo. Los materiales compuestos metal/cerámica, como aluminio/diamante y aluminio/grafito, son buenos ejemplos de disipadores de calor pasivos. Numerosos autores revelaron que las prestaciones de estos materiales pueden ser mejoradas mediante la nanoingeniería interfacial matriz-refuerzo, dando lugar a materiales compuestos de conductividad térmica superior, bajos coeficientes térmicos de expansión y, en ocasiones, propiedades mecánicas mejoradas. Por otro lado, los disipadores activos se encargan de transportar el calor por conducción a través de la estructura sólida del material y transferirlo por convección a un fluido en movimiento a través de su estructura interna que lo elimina al medio. Los disipadores activos más comunes son los conocidos disipadores de aletas de aluminio. En ocasiones, estos son sustituidos por espumas metálicas de poro abierto puesto que presentan una mayor área específica, elevado coeficiente térmico de transferencia, así como una buena conductividad térmica y densidad reducida. La Figura 1 ilustra la arquitectura de un empaquetado electrónico simplificado en el que

se emplea un disipador activo de aletas de aluminio (Figura 1a) y otro en el que el disipador activo es sustituido por una espuma de aluminio (Figura 1b). Así mismo, los mecanismos de transferencia de calor que ocurren durante la operación de estos empaquetados se representan en la Figura 1c y 1d.

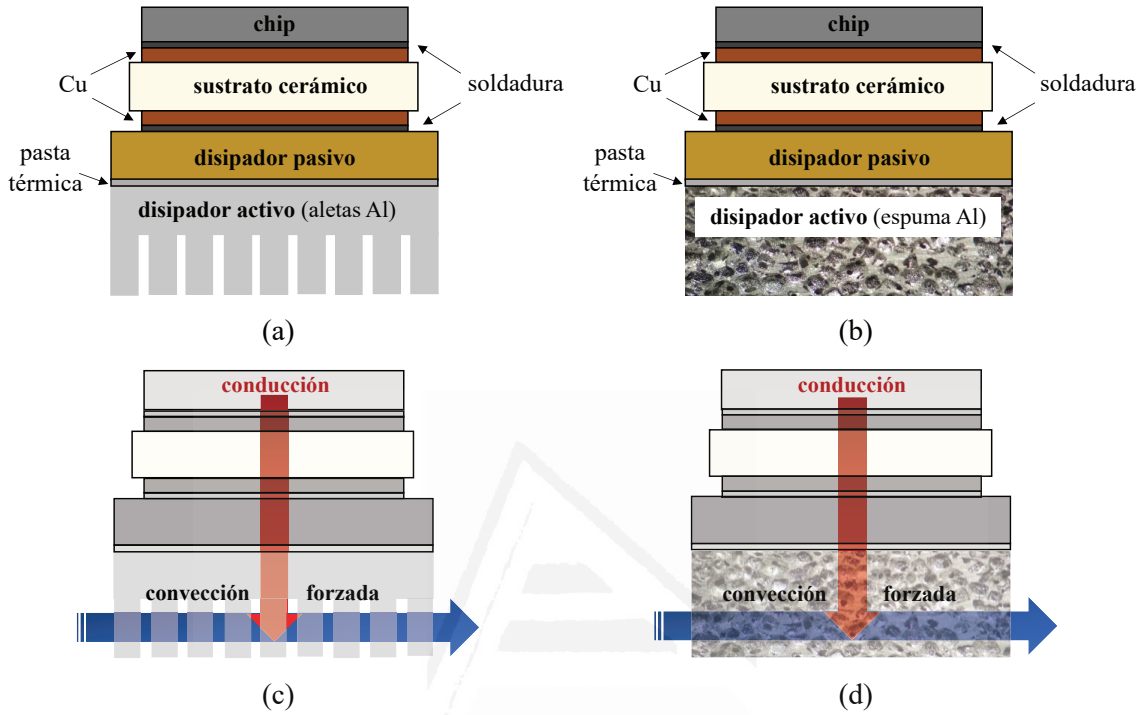

Figura 1. Arquitectura de empaquetados electrónicos (a,b) y mecanismos de transferencia de calor que ocurren en condiciones operacionales (c,d) cuando se emplean diferentes disipadores activos: aletas de aluminio (a,c) o espuma de aluminio (b,d).

Existen dos estrategias para la generación de porosidad en espumas de poro abierto: i) autoformación, según la cual la porosidad se genera mediante un proceso de evolución regido por los principios físicos, y ii) prediseño, donde la estructura se crea de forma más controlada con el uso de moldes mártir que determinan las cavidades porosas. Las técnicas de fabricación de espumas de poro abierto en las que la generación de porosidad se controla empleando una estrategia de prediseño pueden clasificarse en cuatro grupos atendiendo al estado del material precursor: líquido, sólido, vapor e iones. Cuando el material precursor se encuentra en estado líquido, las técnicas de procesado más importantes son la colada a molde perdido de espumas poliméricas y la colada alrededor de partículas o infiltración sobre preformas mártir. Si el procesado se lleva a cabo con un precursor en estado sólido, pueden destacarse técnicas como: sinterización parcial de polvos y fibras, presurización y sinterización de polvos en preformas mártir, sinterización de esferas huecas, sinterización de polvos y aglutinantes, o reacción de sistemas multicomponentes. Así mismo, el

procesado de espumas en estado vapor e iónico concierne la deposición de vapor y electrodeposición, respectivamente, del material precursor sobre espumas poliméricas.

De entre la amplia variedad de técnicas de fabricación, la infiltración de preformas mártir, también conocida como método de replicación, resulta ser la más interesante puesto que permite el mejor control sobre el material. Este método ha sido utilizado tradicionalmente para la obtención de espumas metálicas de poro abierto. El método de replicación, esquematizado en la Figura 2, consiste en producir una preforma porosa, normalmente de partículas empaquetadas, con un agente plantilla (cloruro de sodio, carbón, etc.) que posteriormente es infiltrada con metal fundido o cualquier otro líquido precursor de la matriz para producir un material compuesto. Tras la solidificación del líquido precursor, esta es eliminada o bien por disolución o bien por reacción química controlada (por ejemplo, combustión) para dejar una estructura porosa interconectada que puede ser considerada como el "negativo" de la preforma inicial.

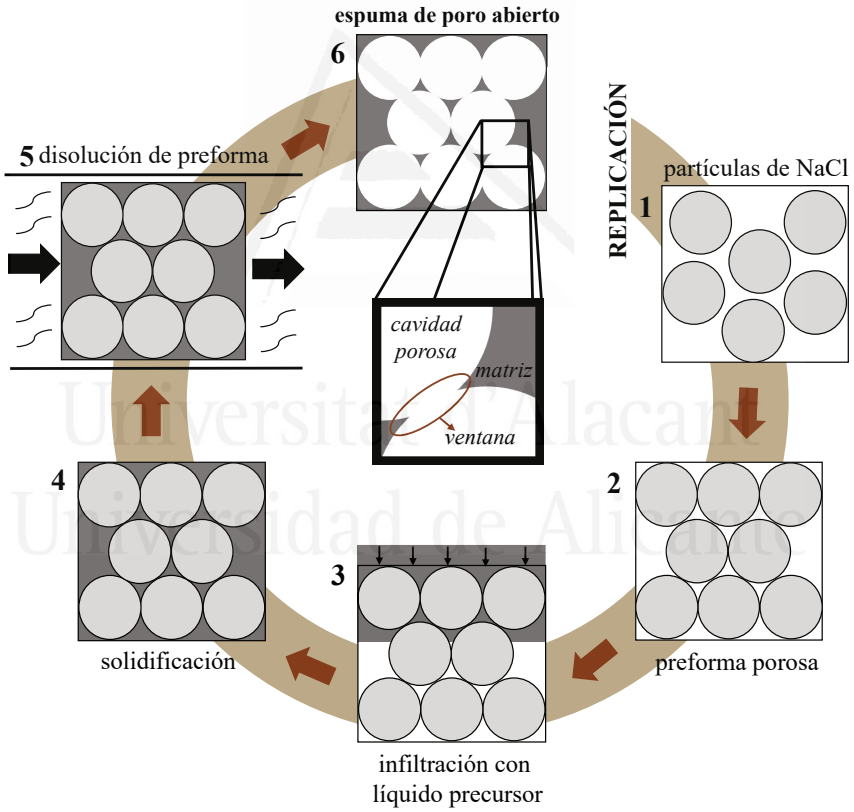

Figura 2. Etapas del procesado de espumas de poro abierto por el método de replicación en el que se emplean partículas mártir de NaCl como agente plantilla.

Este método tiene la ventaja de ser suficientemente versátil como para permitir el control de la fracción de volumen, el tamaño, la forma y la distribución del tamaño de los poros. Con este control preciso, las propiedades de las espumas fabricadas pueden ser ajustadas fácilmente al intervalo deseado. Dependiendo del material precursor y de la arquitectura porosa final deseada, diferentes

materias primas han sido empleadas para la preparación de preformas mártir. No obstante, el material más utilizado es el cloruro de sodio (NaCl) en forma de partículas, que puede ser convenientemente empaquetado e infiltrado con precursores líquidos a temperaturas inferiores a su punto de fusión (801°C) y luego eliminado por disolución en soluciones acuosas. Las espumas metálicas obtenidas por el método de replicación se caracterizan por presentar baja porosidad (menor al 70%), dando lugar a materiales con caídas de presión más elevadas que las espumas metálicas comerciales, pero con una clara ventaja frente a estas: la habilidad de disipar grandes cantidades de flujo de calor como consecuencia de una elevada fracción de volumen de metal.
Una revisión bibliográfica de los últimos años revela que diversos autores han adoptado la estrategia de incorporar nuevas fases a las espumas de poro abierto, ya que parece ser una forma adecuada de superar los requisitos de muchas aplicaciones tales como las estructurales, catalíticas, electroquímicas y biomédicas. Sin embargo, existen escasos antecedentes donde se contemple dicha estrategia para modificar materiales aplicados al control térmico activo. A pesar de los grandes atributos que presentan las espumas metálicas tradicionales utilizadas para disipación térmica, el acelerado crecimiento tecnológico hace que sus prestaciones sean insuficientes para cumplir con los requisitos de los equipos electrónicos más avanzados. Existe, por tanto, la necesidad de reformular sus diseños con el fin de potenciar sus propiedades.

A la vista de dicha problemática actual, surge el desarrollo de la presente Tesis Doctoral, cuyas hipótesis se plantean a continuación:

1. Las espumas metálicas, ampliamente utilizadas para disipación térmica, presentan propiedades que han limitado su uso en las tecnologías emergentes, de modo que sus diseños han de ser reformulados. La estrategia de incorporar nuevas fases en la matriz estructural de las espumas metálicas parece ser la forma más adecuada para ampliar su aplicabilidad.
2. El método de replicación, comúnmente utilizado para la fabricación de espumas metálicas de poro abierto, es suficientemente versátil como para permitir un control sobre la estructura porosa del material final. La utilización de preformas mártir para la generación de porosidad a partir de un agente plantilla, permite que la incorporación de nuevas fases en el empaquetado sea completamente viable, siempre que se tengan en consideración ciertos aspectos de diseño. Ejemplo de ellos son, entre muchos, que las fases incorporadas no rompan la coordinación de las partículas del agente plantilla de tal modo que impidan la eliminación de estas tras la infiltración, evitando así la interconexión entre poros en el material final; o bien que el sistema matriz-inclusión presente una mala interfase térmica y/o mecánica.
3. La utilización de refuerzos de base carbono en materiales compuestos de matriz aluminio, tales como copos de grafito o diamante, han proporcionado conductividades térmicas muy

superiores a los materiales monolíticos análogos, de modo que pueden considerarse como potenciales inclusiones térmicas en espumas metálicas de poro abierto.

4. Puesto que la eliminación de calor en los disipadores activos ocurre por un mecanismo de conducción/convección forzada, los materiales con mayor conductividad térmica serán capaces de conducir el calor de forma más efectiva hasta zonas más alejadas del foco emisor de calor, que posteriormente será transportado por un fluido para eliminarlo al medio. Por ello, se espera que las espumas metálicas de poro abierto con inclusiones térmicas de base carbono den lugar a potencias disipadas superiores en comparación con las espumas metálicas tradicionales.

En base a estas hipótesis, se formulan los siguientes objetivos generales:

1. Desarrollo de espumas de aluminio de poro abierto que contengan copos de grafito como inclusiones térmicas (espumas de material compuesto aluminio/copos de grafito) y evaluación de su aplicabilidad en el campo de la disipación térmica activa.
2. Desarrollo de espumas de aluminio de poro abierto que contengan partículas de diamante como inclusiones térmicas (espumas de material compuesto aluminio/diamante) y evaluación de su aplicabilidad en el campo de la disipación térmica activa.
3. Empleo de la nanoingeniería interfacial con el fin de modificar las propiedades de las espumas de aluminio de poro abierto con inclusiones térmicas de base carbono (copos de grafito y partículas de diamante) y evaluación de su aplicabilidad en el campo de la disipación térmica activa.

Así mismo, los objetivos específicos se enumeran a continuación:

1. Diseño y fabricación de espumas de aluminio de poro abierto que incorporen copos de grafito, haciendo uso del método de replicación y variando la fracción de volumen de las fases presentes.
2. Diseño y fabricación de espumas de aluminio de poro abierto que incorporen partículas de diamante, haciendo uso del método de replicación y variando la fracción de volumen de las fases presentes.
3. Diseño y fabricación de espumas de material compuesto aluminio/copos de grafito y aluminio/diamante con interfases metal-inclusión modificadas, haciendo uso del método de replicación y la nanoingeniería interfacial.
4. Caracterización microestructural de los materiales fabricados, en la que se evalúe la orientación de los copos de grafito, la distribución de las inclusiones en la fase matriz, la morfología y tamaño de las ventanas de interconexión, así como las interfases metal-inclusión generadas.

5. Caracterización fluidodinámica de los materiales fabricados, en los que se evalúe la caída de presión y la permeabilidad de los mismos.
6. Caracterización térmica de los materiales fabricados, contemplando propiedades tales como conductividad térmica y potencia disipada en condiciones operacionales.
7. Evaluación del comportamiento mecánico de los materiales fabricados mediante ensayos de flexión a tres puntos.
8. Empleo de las herramientas de simulación computacional para la modelización térmica de espumas de material compuesto aluminio/diamante y verificación de los resultados experimentales.
9. Evaluación de la viabilidad de los materiales fabricados para su uso como disipadores de calor en aplicaciones de control térmico activo.

El cumplimiento de los objetivos planteados se evidencia en el desarrollo de los siguientes cuatro capítulos. Dos de ellos fueron publicados como artículos científicos en revistas indexadas en Journal Citation Reports - JCR (Capítulo 1 y 3 en el primer cuartil), otro se publicó como capítulo de libro de acceso abierto (Capítulo 2) y el último se encuentra en aras de ser publicado como artículo científico en una revista del primer decil (Capítulo 4). La consecución de todos ellos constituye una unidad temática de alto interés científico-tecnológico, proporcionando un nuevo abanico de aplicabilidad para las espumas de poro abierto en lo referente al control térmico activo. Así mismo, se cree que el desarrollo de los materiales aquí planteados, así como las técnicas empleadas para su fabricación, pueden ser una nueva vía exploratoria para su aplicación no sólo en la industria electrónica, sino también en otras como la biomédica y catalítica.

Capítulo 1. Vencer el reto del control térmico mediante la incorporación de grafito en espumas de aluminio

En el Capítulo 1 de la presente Tesis Doctoral se propone el diseño, la fabricación y la caracterización de una nueva familia de espumas de aluminio de poro abierto con copos de grafito como inclusiones térmicas. Los nuevos materiales fueron inspirados en la unión de dos ideas: el empleo de inclusiones de base carbono como potenciadores de la conductividad térmica y el aprovechamiento de las ventajas fluidodinámicas que proporcionan los materiales con una estructura porosa interconectada. Las ventajas de los copos de grafito (Gf) como inclusiones térmicas incluyen una baja densidad, fácil mecanizado y elevada anisotropía. Esta última repercute en propiedades como la conductividad térmica (1000-2000 $Wm^{-1}K^{-1}$ en el plano basal y 38 $Wm^{-1}K^{-1}$ en el plano perpendicular), el coeficiente térmico de expansión (-1×10^{-6} K^{-1} en el plano, 28×10^{-6} K^{-1} fuera del plano) y el comportamiento mecánico.

Las espumas de material compuesto fueron fabricadas mediante el conocido método de replicación. Para ello, se prepararon preformas porosas que consistían en compactados de cloruro de sodio y copos de grafito orientados y convenientemente distribuidos. Las preformas se infiltraron por presión de gas con aluminio líquido, el cual fue rápidamente solidificado con el fin de evitar la formación de productos de reacción en la interfase metal-inclusión. A continuación, las partículas de NaCl se eliminaron por disolución, obteniéndose dos familias de materiales que difieren en la distribución de las inclusiones en la fase matriz: i) espumas de aluminio con copos de grafito orientados y distribuidos homogéneamente en la matriz y ii) materiales formados por capas alternadas de espuma de aluminio y copos de grafito orientados. Ambas estructuras se representan en la Figura 3.

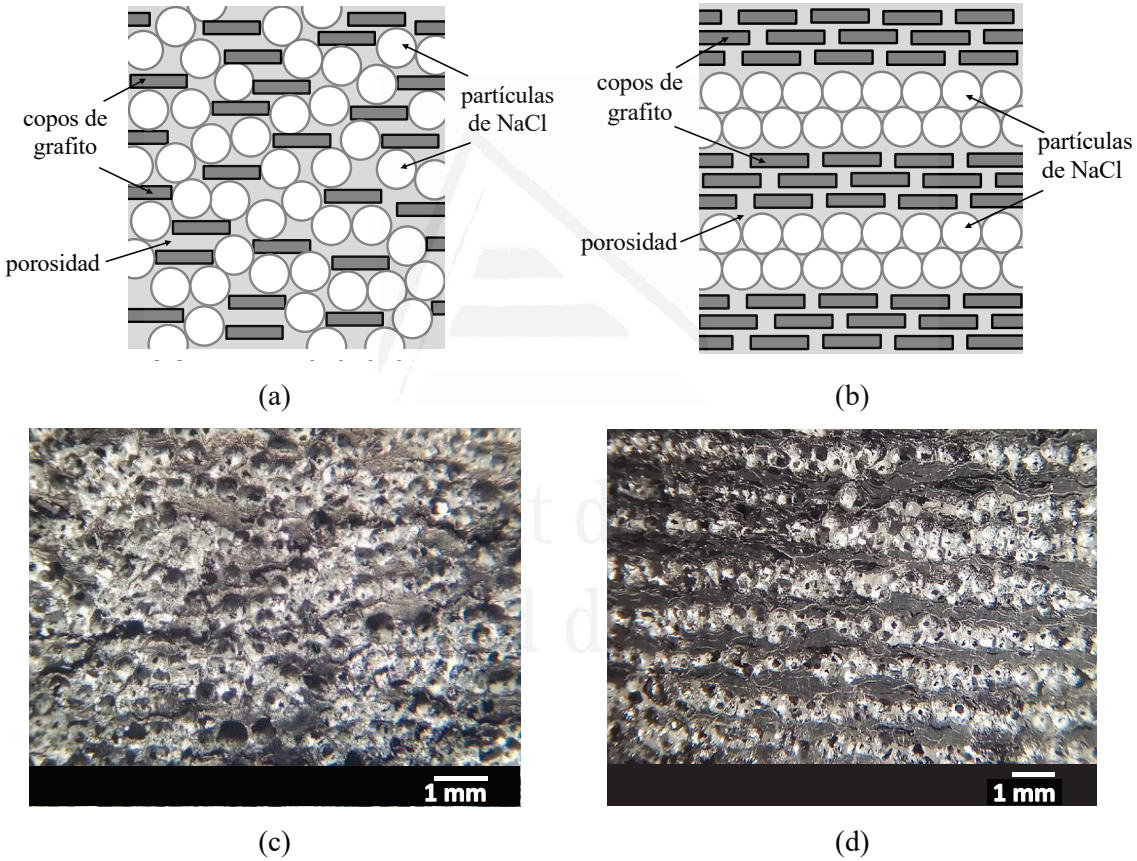

Figura 3. Representación esquemática de las estructuras de las preformas (a,b) e imágenes ópticas de las espumas fabricadas (c,d). (a,c) hacen referencia a espumas de aluminio con copos de grafito orientados y distribuidos homogéneamente en la matriz, mientras que (b,d) a materiales formados por capas alternadas de espuma de aluminio y copos de grafito orientados.

La preparación de preformas porosas, que comúnmente consisten en compactados de partículas de una única naturaleza, tamaño y morfología, resultó ser una etapa crítica en el desarrollo de estos materiales debido de la incorporación de una nueva fase. Con el fin de optimizar el sistema, se llevó

a cabo un estudio exhaustivo sobre el empaquetado de preformas, que contemplaba la utilización de diferentes presiones de compactación, así como la variación de las fracciones de volumen de las fases presentes (NaCl, Gf y poro). Los resultados revelaron que aquellas preformas preparadas a partir de mezclas homogéneas de NaCl y Gf orientados, presentaban dos claras restricciones. La primera de ellas viene determinada por la coordinación de las partículas de NaCl, la cual debe garantizar un proceso de disolución eficaz y completo del agente plantilla y puede entenderse como un límite de percolación. Las partículas de NaCl debían formar una red interconectada con un número de coordinación para cada partícula de al menos 3. En consecuencia, y teniendo en cuenta resultados de otros trabajos publicados, las fracciones de volumen de NaCl estaban limitadas a un valor mínimo de 0.3. La otra restricción conlleva la imposibilidad de fabricar muestras con composiciones determinadas como consecuencia de un empaquetamiento por acción de la gravedad y fue definida como límite de compactación. Esta restricción impide la preparación de preformas de alta porosidad (fracciones de volumen de poro mayores a 0.45) y bajo contenido en Gf (fracciones de volumen de Gf menores a 0.3). En el caso de las preformas en las que los copos de grafito se encuentran formando capas alternadas con los compactados de NaCl, ninguna restricción de percolación es aplicable. En un caso extremo en el que la fracción de volumen de NaCl es tan pequeña comparada con la de Gf que genera capas del espesor de la partícula de NaCl, la coordinación de estas sigue siendo suficiente para ser eliminadas de forma eficaz. Por el contrario, el límite mínimo de compactación también se detectó en este sistema para las preformas preparadas sin presión externa debido a la tendencia natural de las partículas de NaCl y los copos de grafito a colocarse unas encima de otras.

La optimización de los sistemas permitió la fabricación de una serie de materiales que fueron posteriormente caracterizados. Las permeabilidades de las espumas se obtuvieron por métodos experimentales y fueron verificadas mediante un modelo analítico. La aplicación del modelo, soportado por un estudio microestructural que permitió establecer la distribución de tamaños de ventanas de interconexión en las espumas, determinó que los valores de permeabilidad calculados concordaban mejor con los resultados experimentales cuando las ventanas de interconexión consideradas eran las de menor tamaño. Tal y como se esperaba, las espumas presentaban permeabilidades más bajas al disminuir su porosidad. Puesto que la incorporación de copos de grafito en las espumas de aluminio conlleva una disminución de la porosidad global de los materiales, estos generaban caídas de presión al paso de aire forzado superiores a las espumas de aluminio, pero con valores todavía convenientes para las aplicaciones más exigentes en control térmico de la industria electrónica.

Así mismo, se evaluó el comportamiento térmico de los nuevos materiales mediante medidas experimentales de conductividad térmica y potencia disipada en condiciones operacionales utilizando dispositivos diseñados y ensamblados en los laboratorios de la Universidad de Alicante. Las espumas de material compuesto proporcionaron conductividades térmicas longitudinales

excelentes (estando los copos de grafito alineados con el flujo de calor), dentro del intervalo de 60-290 $Wm^{-1}K^{-1}$. Dichos valores fueron predichos con conocidos modelos teóricos que consideraban las dos microestructuras características de ambos tipos de materiales fabricados. Por otro lado, las espumas de material compuesto registraron potencias disipadas de hasta un 325% superior a las de las espumas de aluminio convencionales también fabricadas por el método de replicación.

Además de las prestaciones térmicas, resulta de gran interés conocer la respuesta mecánica de estos materiales ya que suelen estar ensamblados en módulos electrónicos mediante anclajes que imponen una determinada tensión de flexión. Para ello, las espumas fueron sometidas a ensayos de flexión a 3 puntos en una máquina de ensayos universal. Es bien sabido que los copos de grafito son mecánicamente ineficientes cuando se emplean como refuerzo en materiales compuestos de matriz metálica, característica que se trasladó a las espumas aquí fabricadas. Cuando los copos de grafito fueron incorporados a la estructura porosa, los módulos de flexión resultaron ser ligeramente inferiores a las espumas de aluminio, aunque muy superiores a otros materiales espumados empleados para el control térmico activo, haciendo de estos materiales excelentes candidatos para su uso como disipadores de calor.

Capítulo 2. Espumas de poro abierto modificadas por incorporación de nuevas fases: espumas multifásicas para aplicaciones térmicas, catalíticas y médicas emergentes

La incorporación de nuevas fases en la matriz estructural de las espumas de poro abierto ha resultado ser una estrategia empleada por diversos autores para ajustar las propiedades de estos materiales en función de la aplicación deseada. Sin embargo, hasta el desarrollo del presente capítulo, no se encontraba en bibliografía ningún trabajo que reflejara la necesidad de rediseñar estos materiales ni recopilara las diferentes estrategias empleadas para su obtención. El contenido del Capítulo 2 versa sobre las diversas técnicas de fabricación, tanto de las espumas de poro abierto convencionales como de aquellas que incorporan nuevas fases (aquí denominadas espumas multifásicas de poro abierto).

Las espumas multifásicas de poro abierto desarrolladas son todavía escasas y pueden fabricarse por dos métodos bien diferenciados en función de la estructura final deseada. Por un lado, la incorporación de nuevas fases en materiales monolíticos se consigue mediante la precarga de partículas (inclusiones) en la preforma porosa, la precarga de partículas en el líquido precursor de la matriz, o bien por electrodeposición. De este modo se obtienen espumas de material compuesto o espumas con fases huésped alojadas en las cavidades porosas del material, ambas con una dispersión homogénea de las nuevas fases en una matriz continua. El segundo método empleado para la obtención de espumas multifásicas se basa en combinaciones de materiales monolíticos, normalmente caracterizadas por presentar una estructura de capas alternadas. Entre ellos, cabe destacar las espumas de aletas, que se obtienen mediante la unión de monolitos porosos y no porosos

preexistentes (matriz discontinua) o por colada de un líquido precursor en un molde con preformas mártir preexistentes y convenientemente localizadas (matriz continua). En ambos casos, el material no poroso es considerado como la nueva fase. El molde puede contener también preformas mártir alternadas con empaquetados de partículas (inclusiones), dando lugar a espumas de aletas de material compuesto con una matriz continua.

Finalmente, el capítulo recoge los desarrollos de algunos materiales en los que se emplean los métodos anteriormente descritos, diseñados para aplicaciones térmicas, catalíticas y médicas.

Capítulo 3. Guiando el calor en el control térmico activo: Incorporación en un único paso de materiales compuestos de aluminio/diamante con nanoingeniería interfacial en espumas de aluminio

Atendiendo a las excelentes prestaciones de los materiales desarrollados en el Capítulo 1 para disipación térmica activa, se consideró la necesidad de explorar nuevas espumas de material compuesto que incorporasen otras inclusiones térmicas de base carbono. Es bien sabido que las partículas de diamante son ampliamente seleccionadas como refuerzo en materiales compuestos de matriz aluminio para ser utilizados como disipadores pasivos en aplicaciones de control térmico. Estos materiales presentan bajos coeficientes térmicos de expansión y elevadas conductividades térmicas que, además, pueden ser convenientemente ajustadas controlando la reacción en la interfase aluminio-diamante durante su procesado. El presente capítulo expone el diseño, la fabricación y posterior caracterización de materiales espumados que combinan las propiedades de disipación pasiva de los materiales compuestos aluminio/diamante con la elevada capacidad de disipación activa de las espumas de aluminio.

Los nuevos materiales, fabricados por el método de replicación, requirieron de la preparación de preformas porosas que consistían en empaquetados de partículas de NaCl (partículas mártir) y diamante, dispuestos en capas alternadas (Figura 4a). El proceso de infiltración asistida por presión de gas de las preformas porosas con aluminio líquido se controló cuidadosamente con el fin de nano-dimensionar los productos de reacción en la interfase aluminio-diamante. Para ello, se varió el tiempo desde el punto en que se alcanza la máxima presión en la cámara de infiltración. Durante este tiempo (aquí llamado tiempo de contacto), el metal líquido permanece en contacto con las partículas de diamante determinando la reactividad del sistema y, por tanto, la calidad de la interfase generada. En el presente estudio se seleccionaron tiempos de contacto de 0, 15 y 45 minutos. Pasados estos tiempos, el metal fue solidificado y las partículas de NaCl se eliminaron por disolución. Como resultado, se obtuvieron materiales multicomponente estructurados en capas alternadas de componentes de espuma de aluminio y material compuesto aluminio/diamante. La imagen óptica de la Figura 4b expone su estructura representativa. Las diferentes series de

materiales fabricados presentaban una disposición longitudinal o transversal de las capas alternadas de cada componente, así como diferentes relaciones de volumen material compuesto:espuma (27:73, 35:65 y 70:30).

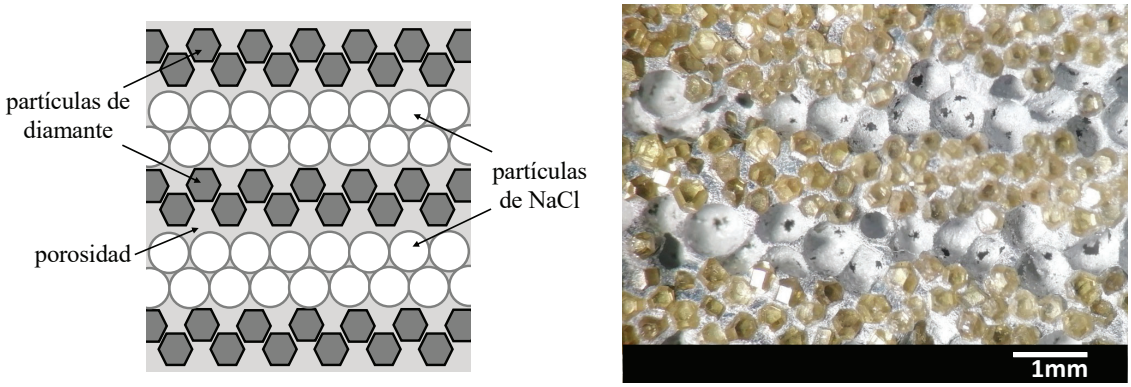

(a) (b)

Figura 4. Representación de una preforma empaquetada consistente en capas alternadas de partículas de NaCl y diamante (a) e imagen óptica de un material multicoponente resultante de la infiltración de una preforma similar a (a) con aluminio líquido.

Del mismo modo que ocurre con las espumas que incorporan copos de grafito, la preparación de los nuevos materiales presenta ciertas restricciones asociadas al empaquetado de partículas en las preformas. Tal como se observó en el Capítulo 1, las partículas de NaCl y Gf pueden ser compactadas en capas alternadas con una presión externa para dar lugar a preformas autosustentables como consecuencia de la flexibilidad de los copos de grafito y las deformaciones locales que pueden sufrir las partículas de NaCl. Esta técnica permite obtener preformas con una amplia variedad de fracciones de volumen de cada fase. Sin embargo, resulta imposible generar preformas autosustentables empleando partículas de NaCl y diamante mediante la aplicación de una presión externa debido a la característica del diamante de ser no deformable. Estas preformas sólo pueden fabricarse en una banda estrecha delimitada por los límites superior e inferior de las fracciones de volumen de empaquetado de las partículas de NaCl (dentro del intervalo 0.58-0.63) y de las partículas de diamante (dentro del intervalo 0.60-0.61). En estos intervalos, los valores inferiores corresponden a la compactación mínima alcanzada por la disposición natural de las partículas cuando se someten a vibraciones. Los valores superiores corresponden al valor de compactación cuando las partículas son cuidadosamente empaquetadas con la ayuda de un pistón manual, permitiendo acomodar “mejor” las partículas.

La caracterización microestructural de los materiales multicomponente se llevó a cabo haciendo uso de la microscopía óptica y la microscopía electrónica de barrido (SEM) permitiendo observar, respectivamente, la estructura global de los materiales y los productos de reacción (cristales de Al_4C_3) en la interfase aluminio-diamante.

El comportamiento térmico de los materiales fabricados se evaluó mediante medidas de conductividad térmica y potencia disipada, haciendo uso de equipos diseñados y ensamblados en la Universidad de Alicante. Los resultados indicaron que las condiciones de procesado afectan a las prestaciones térmicas de los materiales, siendo aquellos que se fabricaron a tiempos de contacto de 15 minutos los que proporcionan mayor conductividad térmica. Los valores de conductividad térmica alcanzaron los 435 $Wm^{-1}K^{-1}$ cuando el material multicomponente presentaba un arreglo longitudinal (la disposición de las capas alternadas era paralela al flujo de calor) y una relación de volumen entre componentes material compuesto:espuma de 70:30. Además, este material proporcionó potencias disipadas en condiciones de trabajo de hasta un 130% superior a la de las espumas de aluminio convencionales también fabricadas por el método de replicación. Los valores de conductividad térmica se discutieron empleando conocidos modelos analíticos que consideran un sistema de capas alternadas semi-infinitas de material compuesto y espuma metálica, mientras que las potencias disipadas se corroboraron mediante modelización con elementos finitos por medio de la herramienta de simulación computacional Ansys-Fuent.

Por otro lado, los materiales se sometieron a una caracterización mecánica mediante ensayos de flexión a 3 puntos con una máquina de ensayos universal. Se determinó que las propiedades mecánicas de los materiales multicomponente escalaban con la conductividad térmica, indicando que la generación de una interfase térmica óptima daba lugar a la mejor interfase mecánica metal-partícula en los componentes de material compuesto. El valor del módulo de flexión para el material optimizado térmicamente resultó ser la mitad de la de un material compuesto aluminio/diamante obtenido bajo las mismas condiciones de procesado y casi 20 veces superior a las espumas de aluminio convencionales. Dado que estas no plantean problemas de fallo por flexión cuando se integran en los empaquetados electrónicos, se puede concluir que los materiales multicomponentes desarrollados en este estudio superan los requisitos mecánicos mínimos de estas aplicaciones.

Los resultados sugieren que la presencia de componentes de material compuesto aluminio/diamante de alta conductividad térmica puede mejorar significativamente la disipación de calor de las espumas de aluminio convencionales, ya que actúan principalmente como guías térmicas eficaces que conducen el calor y lo transfieren a los componentes de la espuma de aluminio donde la disipación se consigue por convección forzada. La elevada transmisión de calor entre capas, causada por la presencia de una matriz metálica continua entre ambos componentes, hace de estos materiales serios candidatos para su aplicación en control térmico activo.

Capítulo 4. Espumas de material compuesto Al/Gf con interfases dimensionadas de SiC para la próxima generación de materiales en disipación de calor activa

Los resultados derivados de los estudios llevados a cabo en el Capítulo 1 y 3 inspiraron el desarrollo del presente capítulo. Este último se centra en la modificación de espumas de material compuesto aluminio/copos de grafito mediante la incorporación de carburo de silicio (SiC) en la interfase metal-inclusión con el fin de mejorar sus propiedades térmicas y mecánicas.

La bibliografía reporta numerosos estudios en los que se emplean copos de grafito como refuerzo de materiales compuestos con el fin de ser utilizados como disipadores pasivos. Sin embargo, las excelentes propiedades de los copos de grafito a menudo no se transfieren a los materiales compuestos finales debido a la débil unión interfacial entre el aluminio y los copos de grafito, que se debe principalmente a la mala mojadura del sistema matriz-refuerzo. Se ha demostrado que la ingeniería interfacial puede mejorar las propiedades térmicas y mecánicas de estos materiales mediante el recubrimiento de los copos de grafito con fases cerámicas como carburos metálicos. Esta idea fue aplicada en el presente capítulo para el desarrollo de espumas de material compuesto aluminio/copos de grafito mejoradas.

Los nuevos materiales se fabricaron mediante el método de replicación. Para ello, se prepararon dos series de preformas porosas diferenciadas por el tamaño medio de las partículas presentes: i) preformas de NaCl de 105 μm que contenían una distribución homogénea de Gf de 150 μm orientados y recubiertos de SiC y ii) preformas de NaCl de 305 μm que contenían una distribución homogénea de Gf de 500 μm orientados y recubiertos de SiC. A continuación, las preformas fueron infiltradas por presión de gas con aluminio líquido empleando un tiempo de contacto igual a cero. Tras la solidificación del metal, el agente plantilla fue eliminado por disolución, dando lugar a espumas de material compuesto con una estructura porosa interconectada. La optimización de la interfase y, por tanto, de las prestaciones de estos materiales, se llevó a cabo empleando Gf con diferentes grados de recubrimiento de SiC. Para ello, se empleó el conocido método de síntesis en sales fundidas variando el tiempo de tratamiento (de 1 a 60 minutos). La Figura 5 detalla la estructura de una preforma preparada para su infiltración con aluminio líquido, así como el proceso de interdifusión que tiene lugar en la interfase Gf-silicio durante el recubrimiento de los copos de grafito.

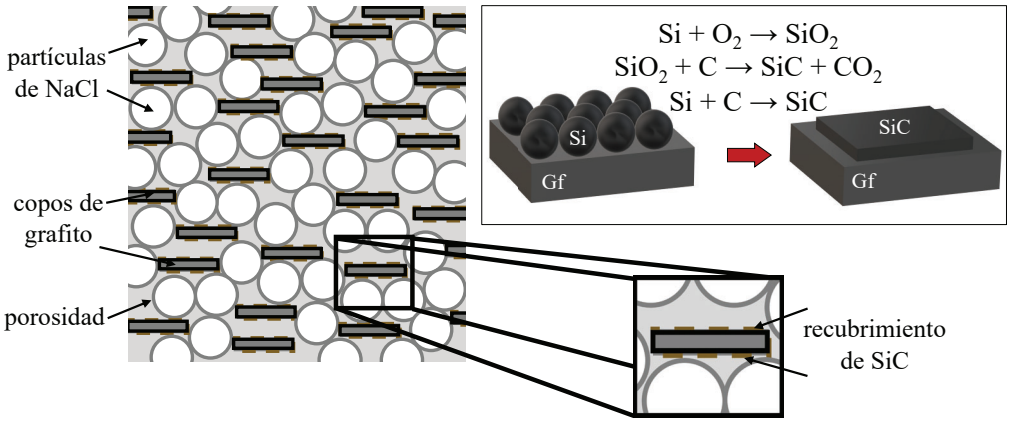

Figura 5. Representación de una preforma de NaCl que contiene copos de grafito recubiertos de SiC orientados y distribuidos homogéneamente y proceso de interdifusión que tiene lugar en la interfase entre los copos de grafito y las partículas de silicio durante el recubrimiento de los Gf con sales fundidas.

La morfología y composición química de los recubrimientos generados sobre los copos de grafito fueron analizadas empleando diversas técnicas de caracterización como microscopía electrónica de barrido (SEM), espectroscopía de rayos X acoplado a SEM (SEM-EDX) y difracción de ratos X (DRX). Los resultados confirmaron que los recubrimientos generados sobre los copos de grafito mediante el método de síntesis en sales fundidas eran de SiC y presentaban discontinuidad, incluso en aquellos casos en los que se emplearon tiempos de tratamiento más prolongados.

Las medidas de caída de presión indicaron que las espumas de material compuesto con poros de mayor tamaño (derivadas del uso de partículas de NaCl grandes) daban lugar a permeabilidades más elevadas. Al igual que en el Capítulo 1, se empleó un modelo analítico que permitió predecir el comportamiento fluidodinámico de los materiales. Dicho modelo, soportado por un análisis microestructural que permitió determinar la distribución de tamaños de ventanas de interconexión, estableció nuevamente que las permeabilidades calculadas se correlacionan mejor con las medidas experimentales cuando se consideran los menores tamaños medios de ventana.

Por otro lado, se evaluaron las prestaciones térmicas de los materiales espumados mediante medidas experimentales de conductividad térmica y potencia disipada en condiciones operacionales. Para ello, se hizo uso de equipos diseñados y ensamblados en los laboratorios de la Universidad de Alicante. La mejor conductividad térmica registrada fue de 232 $Wm^{-1}K^{-1}$ para la espuma que contenía Gf de 500 μm recubiertos durante un tratamiento de 10 minutos y una disposición longitudinal (con los Gf orientados paralelamente al flujo de calor). Así mismo, se comprobó que la disipación de calor del material optimizado era aproximadamente un 500% superior a la de las espumas de aluminio convencionales y un 104% mayor que la de las espumas aluminio/copos de grafito con interfases no modificadas.

Por otro lado, la caracterización mecánica fue llevada a cabo sometiendo los materiales a ensayos de flexión a 3 puntos con una máquina de ensayos universal. Al igual que en los materiales multicomponente presentados en el Capítulo 3, se determinó que las espumas de material compuesto con Gf de 500 μm y la mejor interfase térmica presentaban el mejor comportamiento mecánico de su serie. El módulo de flexión resultó ser del doble que el de una espuma análoga con una interfase no modificada. En su conjunto, los resultados sugieren que este material espumado puede ser considerado un excelente candidato para las futuras generaciones de disipadores de calor activos en electrónica.

Published Works

Chapter 1

Challenging thermal management by incorporation of graphite into aluminium foams

L.P. Maiorano, J.M. Molina. “Challenging thermal management by incorporation of graphite into aluminium foams”. Materials and Design 2018; 158:160-71.

DOI: 10.1016/j.matdes.2018.08.026

ABSTRACT

The recent progress made in active thermal management for electronics demands the development of new open-pore foam materials with excellent thermal performance that result from the combination of high thermal conductivity (≥70 W/mK) and the lowest possible fluid pressure drop. The foams considered to date in the literature do not meet these conditions. In this work, a new class of two-phase composite foam materials, which contain graphite flakes and aluminium, were fabricated by the gas pressure liquid metal infiltration method. These materials were fabricated in two main microstructures: i) aluminium foam with oriented graphite flakes in struts; ii) alternating layers of oriented graphite flakes and aluminium foam. The resulting materials exhibited thermal conductivities within the 60-290 W/mK range, and power dissipation capacities up to 325% higher than those for conventional aluminium foams, with pressure drops kept at convenient values for the most demanding active thermal management applications.

Chapter 2

Open-pore foams modified by incorporation of new phases: multiphase foams for thermal, catalytic and medical emerging applications

Lucila Paola Maiorano Lauria and José Miguel Molina Jordá. “Open-Pore Foams Modified by Incorporation of New Phases: Multiphase Foams for Thermal, Catalytic and Medical Emerging Applications”. Foams - Emerging Technologies, IntechOpen 2019.

DOI: 10.5772/intechopen.88977

ABSTRACT

Recently, open-pore foam materials have acquired great interest in several technological sectors due to their excellent properties of low density, great specific surface area, adjustable thermal conductivity and high-energy absorption. The replication method has proved to be one of the most widely used techniques for their manufacture, allowing a perfect control of the pores’ characteristics from which the main properties of the foams derive. However, these properties have limited the use of these materials in ultimate applications of the most demanding emerging technologies. This chapter reviews recent developments of open-pore foams that have been modified by the incorporation of new phases in order to enhance their properties. The inclusion of new phases taking part of the microstructure or modifying the pore surfaces allow these materials to be considered promising for the most modern applications including, among others, thermal dissipation, catalytic supports and medical implantology.

Chapter 3

Guiding heat in active thermal management: One-pot incorporation of interfacial nano-engineered aluminium/diamond composites into aluminium foams

L.P. Maiorano, J.M. Molina. “Guiding heat in active termal management: One-pot incorporation of interfacial nano-engineered aluminium/diamond composites into aluminium foams”. Composites Part A 2020; 133:105859.

DOI: 10.1016/j.compositesa.2020.105859

ABSTRACT

Traditional metal foams, which are incapable to meet the heat dissipation demands of today’s electronics industry, were recently reformulated by the incorporation of thermal inclusions of graphite flakes that enhance their heat dissipation efficiency. In this work we manufacture, by means of a one-pot liquid metal infiltration synthesis, new layer-structured multicomponent materials that consist of aluminium foam components alternated with aluminium/diamond composite components. The thermal conductivity of aluminium/diamond components can substantially vary with processing conditions, which allow the nano-dimensional control of reaction products at the aluminium-diamond interface. The experimental and analytical results, plus finite element modelling, revealed that the low thermal resistance interface between components derived from the one-pot synthesis route, allowed multicomponent materials to significantly improve the thermal dissipation of traditional foams since aluminium/diamond components acted as effective thermal guides capable of transferring heat to the aluminium foam components where dissipation was achieved by forced convection.

Unpublished Works

Chapter 4

Al/Gf composite foams with SiC-engineered interfaces for the next generation of active heat dissipation materials

1. Introduction

Metal foams with an interconnected porous structure, also known as open-cell metal foams, have been proposed in recent years for a variety of applications. These materials are ideally suited for use as electrodes, catalyst supports, biocompatible and biodegradable structures in biomedical engineering and as heat sinks in different technological fields due to their large surface area per unit volume, low density and high heat transfer capacity [1,2]. The latter application has gained importance in the electronics industry in recent years, as it becomes increasingly important to dissipate the growing amounts of heat generated during the ordinary operation of modern devices. Numerous open-cell metal foams have been investigated for use as active heat sinks due to their ability to dissipate heat by forced conduction/convection [3–8]. Aluminium foams, in particular, have shown significant potential due to their low density and specific thermal conductivity, which is approximately twice that of copper foams. However, to meet the increasingly demanding heat dissipation applications required by the electronics industry, aluminium foams with new incorporated carbon-based phases with improved thermal and mechanical properties have been developed recently [9–11]. In [11], Al/graphite foams were inspired by oriented Al/graphite flake composites developed for use as passive heat sinks [12–17]. The advantages of graphite flakes (Gf) as thermal inclusions include low density, high in-plane thermal conductivity (1000-2000 $Wm^{-1}K^{-1}$ in the basal plane and ≈38 $Wm^{-1}K^{-1}$ in the perpendicular plane [12,13,18]), low thermal expansion coefficient (-1×10^{-6} K^{-1} in-plane, 28×10^{-6} K^{-1} out-of-plane), good mechanical properties and ease of machining [12,17,19,20]. However, the excellent properties of graphite flakes are often not transferred to the final composites because of the week interfacial bonding between graphite and aluminium, which is mainly caused by the poor wettability of the Al/graphite system [21]. It has been shown that interfacial engineering can improve the thermal and mechanical properties of these materials, either by controlling the chemical reaction between graphite and aluminium during fabrication [14] or by pre-coating graphite flakes with certain ceramic [18,20,22] or metallic [23,24] phases. According to [20], SiC-coated Gf-reinforced aluminium composites exhibited better thermal and mechanical properties than the ones containing uncoated Gf. On the other hand, the use of TiC-coated Gf reinforcements in aluminium matrix materials resulted in improved mechanical properties at the expense of a significant reduction in thermal conductivity. Chen et al. [25] discovered that copper matrix composites with Ni-coated Gf outperformed Gf-containing composites without interface treatment in terms of mechanical properties and thermal expansion coefficient. Coatings are generated in a variety of ways in the listed works, with the molten salt synthesis method being particularly popular for SiC or TiC ceramic coatings [20,22,26–28].

The aim of this work is to develop new foams by infiltrating liquid aluminium into NaCl templating preforms (replication method) with SiC-coated graphite flake inclusions. These materials, inspired by those developed in [11], incorporate engineered interfaces to improve their

thermal and mechanical properties, thus extending their range of applications. Different techniques were used to characterize the developed materials, including image analysis, optical microscopy, SEM-EDX and XRD. The mechanical and thermal properties of the materials were also evaluated as a function of their Gf size, SiC-engineered interface and anisotropy (by 3-point bending, thermal conductivity and power dissipation measurements). The composite foam containing larger-sized Gf coated with SiC at 1100 ºC for 10 minutes has the best thermal interface, resulting in the highest thermal conductivity (232 $Wm^{-1}K^{-1}$) and power dissipation capacity, which is almost 500% higher than conventional aluminium foams or 104% higher than Al/graphite foams with uncoated Gf. This material has also an excellent mechanical performance, which is more than twice higher than that of a material with an unmodified interface, making it outstanding for use as an active heat sink in electronics.

2. Experimental procedure

2.1. Materials

High purity aluminium (99.999 wt%), graphite flakes of 10 mesh (99.99% wt%) and crystalline silicon powder with an average size of 325 mesh (99.5 wt%) were supplied by Alfa Aesar (GmbH & Co KG - Karlsruhe, Germany). Analytical grade sodium chloride particles (99.5 wt%) were purchased from Panreac Química S.L.U. (Barcelona, Spain). The graphite flakes and salt particles were sieved to provide various size fractions, which were kept for the preparation of the preforms (see Table 1). Calcium chloride particles with a purity of 99.99% were supplied by the same producer. Representative morphologies of NaCl and graphite flake particles employed in this study are depicted in Figures 1a-c.

2.2. Graphite flakes coating

SiC-coated Gf were prepared by the molten salt synthesis method described in [22]. Graphite flakes, $CaCl_2$ and Si powder in a weight ratio of 5:5:1 were placed in a closed vessel and physically stirred at 60 rpm for 15 minutes using a rotary drive (Stuart STR4, Staffordshire, UK). The mixture was afterwards transferred to an alumina crucible and placed in an argon-filled tube furnace. The heat treatment applied consisted of three sequential steps: heating up to 1100 ºC at a heating rate of 5 $ºCmin^{-1}$, holding this temperature constant for a varied time (1, 10, 30 and 60 minutes) to obtain various degrees of surface coating, and cooling to room temperature. The surplus $CaCl_2$ was then eliminated by dissolving it in distilled water. Finally, the Gf were washed with acetone to remove impurities before drying for 24 hours at 60 °C.

2.3. Fabrication of Al foams and Al/Gf composite foams

Foam materials were manufactured following the replication method [29]. The development of porous preforms is the first step in the fabrication process. For this purpose, physical stirring was used to mix 56 vol% NaCl particles with 44 vol% Gf (Gf were either coated or uncoated, depending on the desired final material) at the same conditions as described in the preceding section (60 rpm for 15 minutes using a rotary drive). The mixtures were placed in a 50 × 30 mm mould and gently vibrated for 10 seconds to achieve proper Gf orientation. A pressure of 0.7 MPa was then applied in the direction perpendicular to the orientation of the Gf using a manual hydraulic press (Figure 1d). As a result, self-standing NaCl preforms with uniformly distributed and oriented graphite flakes were obtained. For comparison, NaCl preforms were prepared in the absence of Gf with the same compaction pressure.

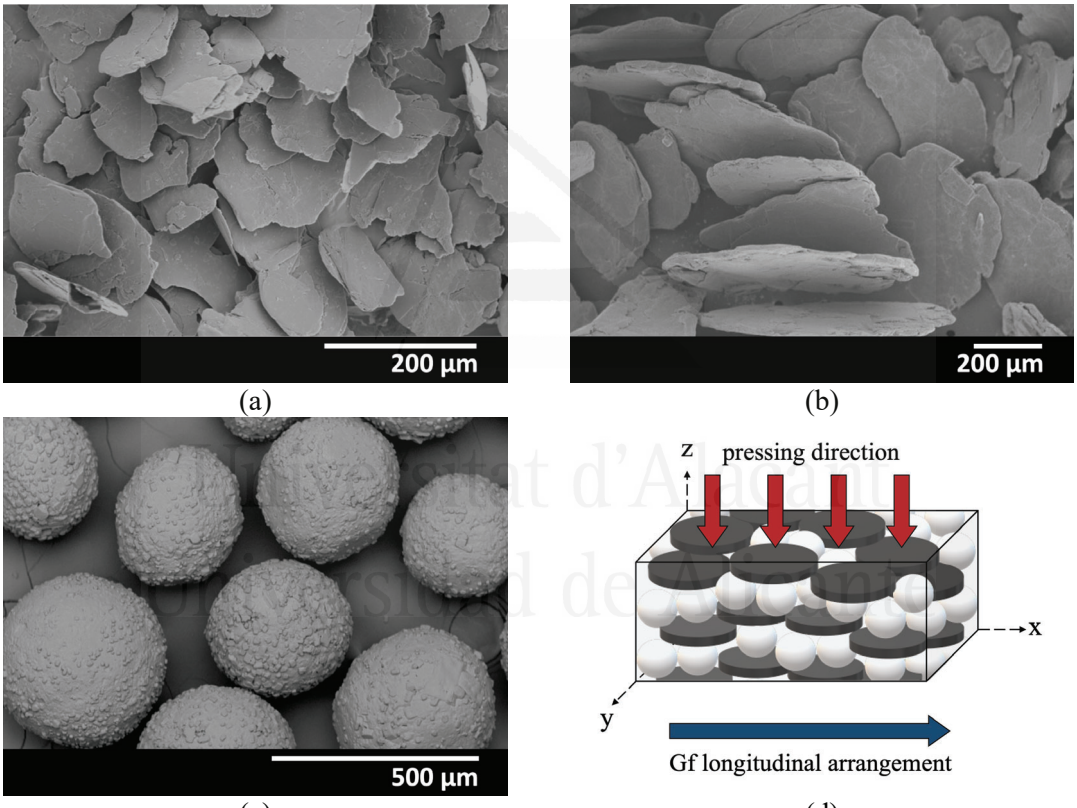

Figure 1. Scanning electron microscopy (SEM) images of 150 µm Gf (a), 500 µm Gf (b) and 315µm NaCl (c) particles used in the fabrication of the composite foams. The schematic drawing in (d) shows the pressing direction (z-axis) of the preforms, which is perpendicular to the orientation plane (x-y plane) of the Gf.

Table 1. Particle sizes and manufacturing conditions for the developed foam materials. D_{Gf} and D_{NaCl} are the average diameters (in μm) of the Gf and NaCl particles, respectively. t_c refers to the time (in minutes) that the preforms and liquid aluminium were in contact, and t_{TT} refers to the coating treatment time (in minutes) of Gf.

Material	Code	D_{Gf}	D_{NaCl}	t_c	t_{TT}
Al foams	A-1	-	105	-	-
	A-2	-	315	-	-
Al/Gf composite foams	B-1	150	105	0	0
	B-2				1
	B-3				10
	B-4				30
	B-5				60
	C-1	500	315	0	0
	C-2				1
	C-3				10
	C-4				30
	C-5				60
	D-1 (B-1)	150	105	0	0
	D-2			5	
	D-3			15	
	D-4			30	
	D-5			45	
	E-1 (C-1)	500	315	0	0
	E-2			5	
	E-3			15	
	E-4			30	
	E-5			45	

In the following step of the fabrication process, the porous preforms were gas pressure infiltrated with liquid aluminium. Each preform was placed in a quartz tube with an inner diameter of 60 mm and a length of 100 mm that had previously been coated with graphite paint (Condat Lubrifiants, Chasse-sur-Rhône, France) to facilitate demoulding. The preform was anchored in the tube using NaCl particles to prevent movement or floating during metal infiltration. A solid aluminium block was placed on the preform and the tube was inserted into a gas pressure infiltration chamber. A vacuum of 0.2 mbar was applied to prevent the formation of uncontrolled porosity due to air trapping during infiltration. The chamber was heated to 750 °C at a heating rate of 5 $^{o}Cmin^{-1}$ and the vacuum was closed after 10 minutes at constant temperature. After that, the chamber was pressurized to allow the liquid metal to penetrate the porous preform. Argon pressures of 9 or 11 bar were employed for preforms having 500 or 150 μm Gf, respectively. The time during which liquid aluminium and graphite flakes are in contact (hereinafter called contact time -tc-) was carefully tracked. Later, the metal was solidified directionally by immersing the chamber from below in a cold-water bath with a high cooling rate (400 $^{o}Cmin^{-1}$). The sample was then extracted and machined to remove the surrounding excess Al/NaCl. Since the composite

foams exhibit anisotropy, samples were cut into differently oriented pieces to perform the various characterizations described in each of the following sections.

The removal of the NaCl preform is the final step of the fabrication process. For that, the procedure described in [11] was employed. This consists of two consecutive steps: first, the sample was immersed in distilled water for 15 minutes while being magnetically stirred to remove the salt present in the outermost part of the material; second, the material was infiltrated with pressurized distilled water to remove the salt present in the inner part of the sample. As a result, a material with an interconnected porous structure that replicates the original preform was obtained. Table 1 collects the numerous materials produced, as well as the conditions under which they were fabricated.

2.4. Characterization of SiC coatings and foam materials

2.4.1. Microstructural characterization

A SEM-Hitachi S3000N scanning electron microscope with variable voltage was used to study the evolution of the reactive product on the Gf surfaces over time. Their compositions were analysed using the same microscope, which had a Bruker XFlash 3001 X-ray detector for map analysis (EDX) and by X-ray diffraction (Bruker D8-Advance). The scanning was performed with monochromatic Cu-Ka radiation at 2θ between 20 and 80º.

In addition, the samples were inspected with a scanning electron microscope (SEM-Hitachi S3000N) and an optical microscope (Olympus PME3-ADL). The orientation degree of Gf incorporated in the metal foam was quantitative evaluated using image analysis software (Buehler-Omnimet Enterprise, Illinois, USA) on 1-µm diamond-finish polished samples.

2.4.2. Pressure drop

Pressure drop measurements were performed by following the air flow through the foam materials, using a setup inspired by [4]. Two ±0.001 bar precision pressure gauges were positioned in two control chambers and were linked at both ends of the sample by 1 m long polymer coiled tubing. The sample was wrapped in a heat-shrinkable polymer tube before being joined to the coiled tubes (for such measurements, the samples were chopped into 20 × 10 × 10 mm parallelepipeds). A ±0.1 $lmin^{-1}$ air flow meter (KiKey Instruments, Trevose, UK) was used to monitor the inlet air flow in the rage 0-15 $lmin^{-1}$. The pressure drop across the foam materials is given by the Darcy-Forchheimer's equation, which takes into account the viscous term of Darcy's law as well as the inertial effects caused by flow in a porous media:

$$\frac{\Delta P}{\Delta L} = \frac{\mu}{k} v + \rho C_2 v^2 \quad (1)$$

where $\Delta P/\Delta L$ is the pressure drop across the foam material, v is the superficial velocity and μ and ρ are the dynamic viscosity and density of the fluid, respectively. The viscous loss (first term on the right-hand side of Equation (1)) is assumed to be linear with velocity and contains the viscous resistance coefficient 1/k, which was used to compute the permeability (k). The inertial term (second term on the right-hand side of Equation (1)) incorporates an inertial resistance coefficient C_2 to account for the nonlinear behaviour of pressure as a function of fluid flow.

2.4.3. Thermal conductivity and power dissipation

Thermal conductivity measurements were carried out in accordance with the International Standard ASTM E-1225-04, using an experimental setup based on a relative steady-state (equal-flow) technique. Each 20 × 10 × 10 mm piece of foam was placed between two blocks. The upper section of the sample came into contact with a brass reference block connected to a 70 °C water bath, while the lower section came into contact with a block chilled by a room temperature water flow. Five thermocouples were used to determine the temperature gradients, three of which were connected to the brass reference and the other two to the sample.

The power dissipation was experimentally determined using a setup developed in the laboratories of the University of Alicante for the simulation of active heat sinks in real-world settings [10,11,30]. The setup forces air through the foam material, which is in contact with a hot surface at its base. This method allows the air to remove heat that has been transmitted by conduction from the hot surface to the foam via convection. The device is equipped with two thermocouples inserted in a brass base, t_1 (set to a constant temperature of 80 ºC) and t_2 (which measures the temperature variation). The brass conducts heat from the heating system to the sample. The air flow rates ranged from 2.5 to 15 $lmin^{-1}$ and were monitored with a ±0.1 $lmin^{-1}$ flow meter. The temperature gradient in the brass base can be linked to the power dissipation P (Wm^{-2}) of the sample using the following equation:

$$P = \frac{K_{ref}(T_2 - T_1)}{\Delta x} \quad (2)$$

where K_{ref} is the thermal conductivity of the brass (assumed to be 109 $Wm^{-1}K^{-1}$ here), T_1 and T_2 are the temperatures measured with thermocouples t_1 and t_2, respectively, and Δx is the distance between them (36 mm).

2.4.4. Flexural modulus

The flexural moduli of the foam materials were determined using an Instron-4411 universal machine to perform 3-point bending tests on specimens of 50 × 20 × 10 mm. The measurements were obtained with the supports spaced 30 mm apart and the crosshead speed set to 0.1 $mm.min^{-1}$.

3. Results

3.1. Chemical and morphological investigation of SiC coatings

Scanning electron microscopy (SEM) images of 500 μm Gf coated by the molten salt synthesis method at 1100 ºC and different treatment times (t_{TT}= 1, 10, 30 and 60 min) are shown in Figure 2. By comparing micrographs of untreated and coated Gf, it is clear that the SiC coating alters the surface morphology by increasing roughness and producing the appearance of surface steps. These changes do not cover the entire surface of the graphite flakes, suggesting that SiC formation is not uniform even at the longest treatment time (t_{TT}= 60 min). These results are in line with those reported in [22], obtained under the same experimental conditions and for which the authors claim continuous coatings despite showing micrographs in which there is manifest discontinuity in the degree of SiC coverage on graphite flakes. Discontinuous SiC coatings on graphite flakes were also found by Wand et al. [19] using a mass ratio of Gf:Si:$CaCl_2$ of 6:6:1 and heating the mixture at 1050 °C for 2 hours in an induction furnace. Despite the obvious discontinuity in the coating, the authors sized the SiC layer in the nanometre range. In [26], where SiC was grown on graphite flakes by a molten salt synthesis method using KCl and NaF, the authors demonstrated that the amount of SiC coating formed depends on the temperature and Si/Gf molar ratio, so that even under the most demanding conditions (1300 °C for 6 hours and Si/Gf molar ratio=1/2) the SiC coatings were not completely continuous. It is therefore to be expected that the SiC growth in this work is not continuous, given that the working conditions are a Si/Gf ratio of about 1/12, temperatures of 1100 °C and treatment times up to one hour.

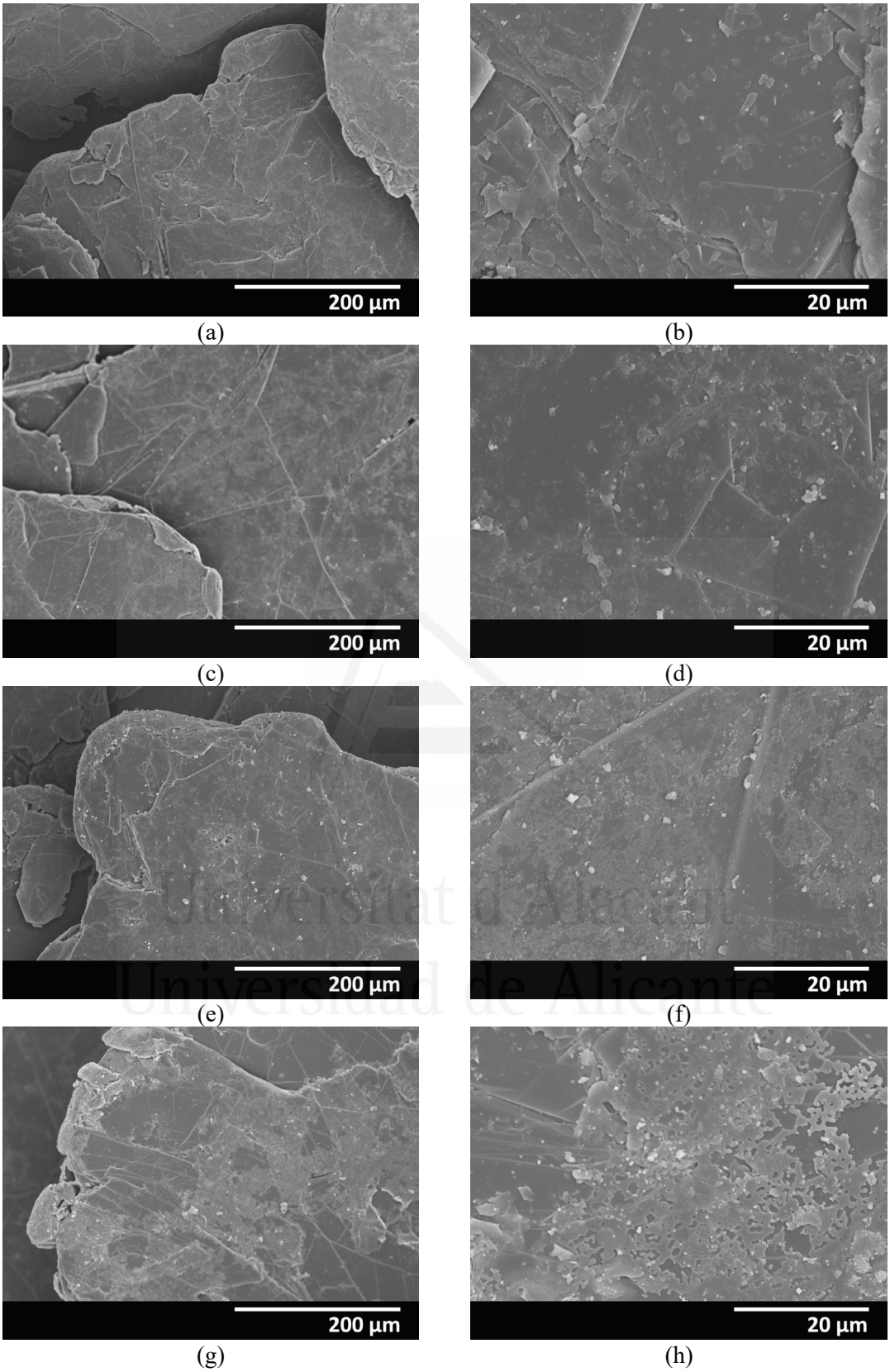

Figure 2. Scanning electron microscopy (SEM) images of SiC-coated Gf with an average diameter of 500 µm, obtained at 1 (a,b), 10 (c,d), 30 (e,f) and 60 (g,h) minutes of coating treatment.

Table 2. EDX analysis of the surfaces of Gf in the original state and SiC-coated Gf with a diameter of 500 µm after a 60-minute coating treatment.

Particles	Element	Weight%	Weight error%	Atomic%
Uncoated Gf	C	90.84	9.6	92.15
	N	8.15	1.3	7.09
	O	0.99	0.2	0.75
	Si	0.02	0.0	0.01
Gf coated at t_{TT}= 60 min	C	68.89	7.7	76.24
	O	25.38	3.1	21.08
	Si	5.51	0.3	2.61
	Ca	0.22	0.0	0.07

To support the observations from the SEM micrographs, a SEM-EDX analysis of the Gf surface in its original state and the SiC-coated Gf surface after a 60-minute coating treatment was performed. The results, listed in Table 2, show that the uncoated Gf, unlike the modified Gf at 60-minute coating treatment, contains virtually no Si. The presence of nitrogen is most likely due to its adsorption in the presence of air. Calcium may be present as a result of the salt used during the coating process. In addition, the coating contains a significant amount of oxygen as a result of the highly oxidizing conditions of the molten salt synthesis method. The interdiffusion process at the graphite-silicon interface during coating treatment is depicted in Figure 3 and leads to the reaction Si + C = SiC [20,22,26]. When Si is exposed to air, a trace amount of SiO_2 is formed, which subsequently may react with the Gf surface to produce SiC via the reaction C + SiO_2 = SiC + CO_2, as shown in the figure.

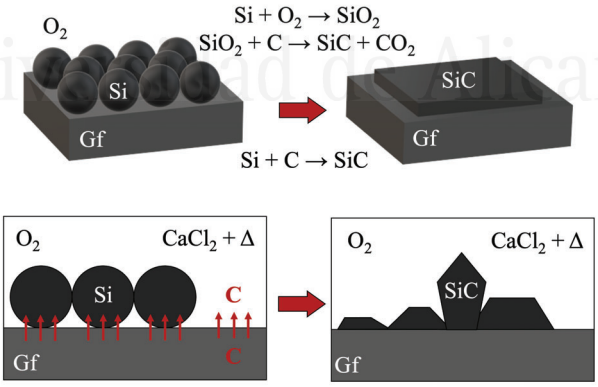

Figure 3. Schematic representation of the interdiffusion process occurring at the interface between Gf and silicon particles during the molten salt coating synthesis.

Figure 4 depicts the X-ray diffraction (XRD) pattern obtained from the analysis of 500 µm SiC-coated Gf treated at t_{TT}= 60 min. The strong graphite diffraction peaks revel that this is the dominant phase. Characteristic beta-SiC peaks appear at 2θ= 35.64º, 60.0º and 71.8º,

corresponding to the cubic beta-SiC diffraction planes (111), (220) and (311), respectively. Moreover, the absence of pure Si peaks is compatible with the entire conversion of Si to SiC.

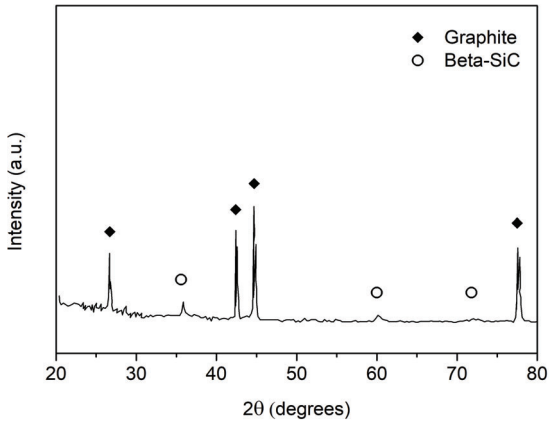

Figure 4. XRD pattern of the 500 μm SiC-coated Gf at t_{TT}= 60 min.

3.2. Microstructure of foam materials

Since the foam materials are the "negative" of the preforms, the volume fractions of sodium chloride (V'NaCl) and pores (V'p) in the preform are virtually equal to the volume fraction of pores (V'p) and metal (V'm), respectively, in the foam. Considering the volume of the final particles packings, as well as its mass and density (2.16 gcm^{-3} for NaCl and 2.26 gcm^{-3} for Gf), the composite foams had pore, Gf and metal volume fractions of 0.47, 0.35 and 0.18, respectively. Likewise, Al foams presented pore and metal volume fractions equal to 0.70 and 0.30, respectively, with an estimated error of ±0.02 in all cases. The materials produced and their specific properties are summarized in Table 3.

Figure 5a shows the geometry of an aluminium foam with SiC-coated Gf (sample B-3), while Figure 5b depicts its representative microstructure. This microstructure reveals details that are crucial for understanding the properties of these materials. On the one hand, the presence of interconnecting windows between the pores is indicative of an open-cell foam. According to [31,32], the processing conditions determine the size and shape of these windows. On the other hand, Figure 5b shows a homogeneous distribution of Gf that appear to be oriented perpendicular to the axis of the uniaxial pressure applied during preform manufacturing. Despite this global orientation, the Gf are not completely aligned in the plane. This is due to flake deformations caused by the fact that some of them enclose the NaCl particles during the pressing stage, resulting in a somewhat curved shape. Figures 6c and 6d show highly magnified SEM images of foams containing uncoated Gf (sample B-1) and SiC-coated Gf at t_{TT}= 10 min (sample B-3) produced at zero contact time. According to [11], metal-free voids occur between uncoated Gf employed as inclusions in aluminium foams because the infiltration pressures used cannot push the liquid aluminium into such narrow slits since the Al/graphite system is non-wetting and thus does not

exhibit spontaneous infiltration (Figure 5c). When Gf are coated with SiC, the spaces between them appear to be filled with metal (Figure 5d). This is most likely because the presence of SiC on Gf enhances the wetting of Gf by liquid aluminium [15]. In fact, the contact angles measured for the Al/SiC system are smaller than those for the Al/graphite system over the entire time interval used to study the spreading kinetics of these systems [21].

Table 3. Properties of the fabricated foam materials: volume fractions of pores, graphite flakes and metal (V´p, V´f and V´m, respectively, with an estimated error of ±0.02), density (ρ, with an estimated error of ±3%), permeability (k, with an estimated error of ±10%) and thermal conductivity in the longitudinal arrangement -parallel to the Gf basal plane- (K^L) and transversal to the Gf basal plane (K^T), each with a ±5% inaccuracy.

Code	**V'p**	**V'f**	**V'm**	**ρ (gcm^{-3})**	**k (m^2)**	**K^L (Wm^1K^{-1})**	**K^T ($Wm^{-1}K^{-1}$)**
A-1	0.70	0	0.30	0.79	1.10×10^{-12}	38	38
A-2				0.77	2.50×10^{-11}	37	37
B-1	0.47	0.35	0.18	1.11	1.91×10^{-12}	148	24
B-2				1.09	-	152	25
B-3				1.11	1.88×10^{-12}	182	28
B-4				1.10	-	169	26
B-5				1.11	-	160	26
C-1	0.47	0.35	0.18	1.09	1.10×10^{-11}	205	25
C-2				1.11	-	216	26
C-3				1.12	9.84×10^{-12}	232	27
C-4				1.11	-	219	26
C-5				1.10	-	218	25
D-1 (B-1)	0.47	0.35	0.18	-	1.91×10^{-12}	148	-
D-2				-	-	154	-
D-3				-	-	158	-
D-4				-	-	157	-
D-5				-	-	156	-
E-1 (C-1)	0.47	0.35	0.18	-	1.10×10^{-11}	205	-
E-2				-	-	208	-
E-3				-	-	210	-
E-4				-	-	209	-
E-5				-	-	208	-

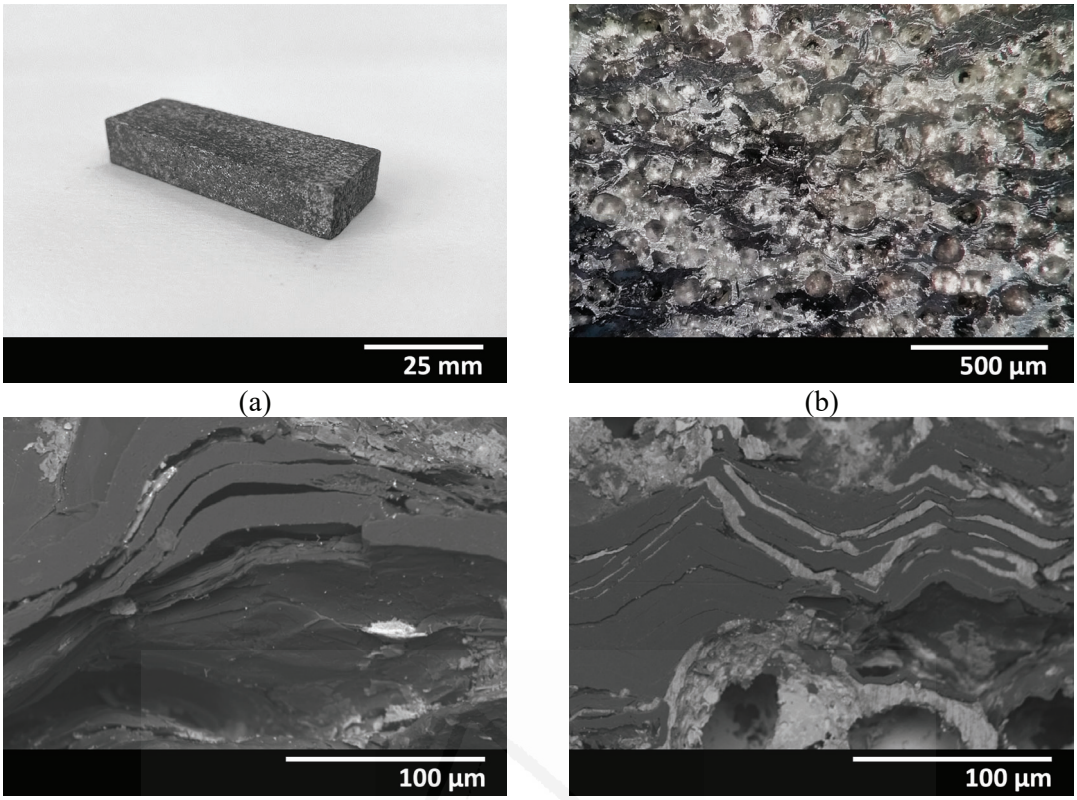

Figure 5. Photographs of the B-3 sample's geometry (a) and its microstructure (b); (c-d) are SEM images of samples B-1and B-3 showing lack and presence, respectively, of aluminium between the spaces left by the Gf.

Figure 6a displays a detail of the pores and pore-connecting windows of sample C-3. The shape of the leachable sodium chloride particles used to make the preforms determined the quasi-spherical geometry of the pores. The pore-connecting windows, which provide interconnectivity in the pore space, are caused by a lack of metal filling in the regions around the contact sites between the NaCl particles at the infiltration pressures used due to the non-wetting behaviour of the Al/NaCl system. Given the well-defined geometry of the NaCl particles, these windows have a fairly uniform, quasi-circular shape. Their average size is governed by a number of variables, including the size of the NaCl particles, the packing pressure, the mechanical properties of the preform being packed, the intrinsic properties of the metal in the liquid state, the wetting characteristics of the metal-particle interface and the infiltration pressures used. The size distributions of these windows are depicted in Figure 6b for samples A-1, A-2, B-3 and C-3. A significant conclusion is derived from this figure: the presence of Gf particles not only reduces the average window size diameter (d_w), but also broadens its size distribution. It appears that the Gf particles interpose themselves between the NaCl particles, preventing them from settling properly. This precludes the high densities observed in the absence of Gf, resulting in smaller and less homogeneous contact zones between NaCl particles, giving rise to pore connecting windows

with broader distributions and shifted to smaller diameters. In addition, there is another consequence: the interposition of Gf between the NaCl particles disrupts their contacts, causing them to lose coordination (see next section for quantitative details).

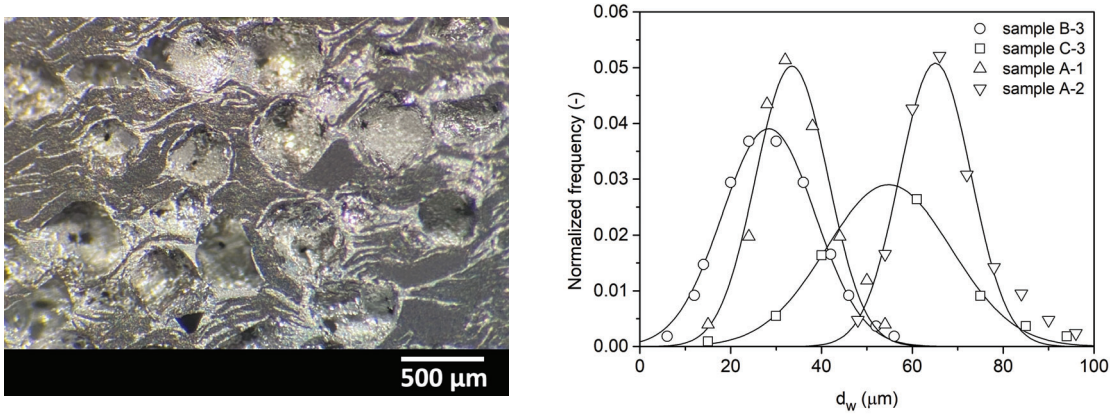

(a) (b)

Figure 6. Photograph showing the pores and pore-connecting windows in sample C-3 (a) and windows size distributions (b) of samples A-1, A-2, B-3 and C-3.

3.3 Pressure drop and permeability - experiments and modelling

Figure 7a shows the relative pressure drop of certain materials studied here as a function of superficial velocity, measured using the experimental setup described in Section 2.4.2. The essentially equivalent fluid-dynamic properties developed in their respective materials imply that Gf, coated or uncoated, results in comparable microstructures (Table 3). A thorough optical microscopy examination demonstrates that the NaCl particles have a coordination number of roughly 5, which is consistent with values reported in [11] for materials with similar microstructures. This coordination number is lower than that of ordinary aluminium foams (about 8-9) because Gf breaks the high coordination number of NaCl particles in the preform. As a result, lower pore-connecting windows densities are expected in Gf-containing preforms, as well as larger pressure drops. The quadratic fit of the $dPdL^{-1}$ vs. v curves follows the Darcy-Forchheimer expression (Equation (1)), which can be used to calculate the permeability values of the materials (these values are given in Table 3). The permeability of replicated foams (foams with porous bottleneck structures and pore-connecting windows) is related to structural parameters by the following equation [34]:

$$k = \frac{V'p \cdot N \cdot {d_w}^3}{24 \cdot \pi \cdot D_p} \tag{3}$$

where N is the coordination number and d_w and D_p are the window and pore diameters, respectively. The mean, minimum and maximum permeabilities of the foams were estimated

(Figure 7b) using V'p=0.47, N=5 and a mean pore diameter of 105 or 315 μm for materials prepared with small and large NaCl particles, respectively, and the mean, minimum and maximum values of d_w (see Figure 6b). Permeabilities appear to be governed by smaller pore-connecting windows, as it was already reported by Maiorano et al. in [11].

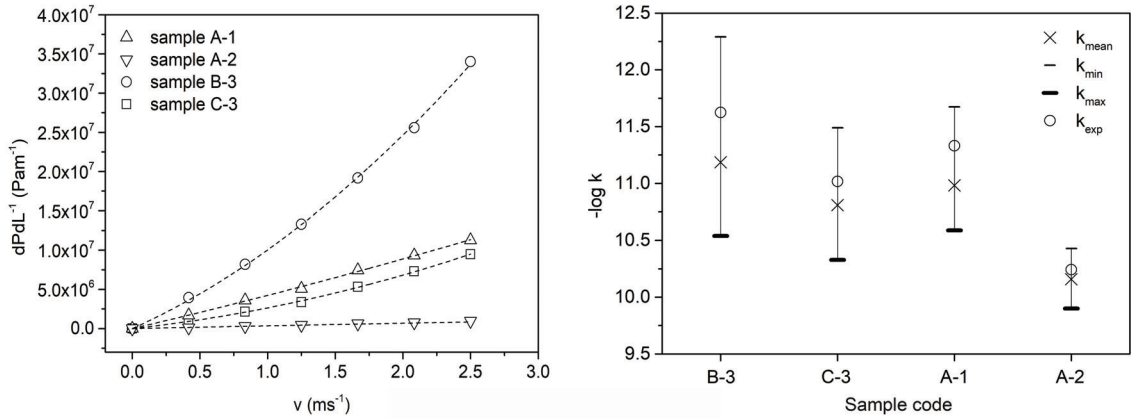

(a) (b)

Figure 7. (a) Pressure drop (dP/dL) of some foam materials as a function of air velocity (v) and their second-degree polynomial fittings for: sample A-1 ($y=2.02\times10^5x^2+4.03\times10^6x$; $R^2=9.99\times10^{-1}$), A-2 ($y=2.64\times10^4x^2+3.15\times10^5x$; $R^2=9.98\times10^{-1}$), B-3 ($y=2.29\times10^6x^2+7.75\times10^6x$; $R^2=9.99\times10^{-1}$) and C-3 ($y=7.72\times10^5x^2+1.87\times10^6x$; $R^2=9.99\times10^{-1}$). The estimated error for pressure drop measurements were found to be of 10%. (b) is a plot representing both experimental and calculated permeabilities (k). k_{mean}, k_{min} and k_{max} are the permeabilities obtained with Equation (3) for $d_w$mean, $d_w$min and $d_w$max.

3.4. Thermal conductivity- experiments and modelling

Thermal conductivity is a property highly dependent on the nature of the interface. The Al/diamond system, which is a chemically reactive system analogous to aluminium/graphite, has been extensively studied in the literature. The formation of a discontinuous interface of aluminium carbide crystals by direct reaction between infiltrating liquid aluminium and packed diamond particles resulted in a significant increase in thermal conductivity of composite materials of approximately 55 percent [10,33]. It seems therefore convenient to investigate, in the composite foams at hand, the effect on thermal conductivity of the aluminium carbide interface generated by the reaction of liquid aluminium and uncoated Gf (Figure 8a).

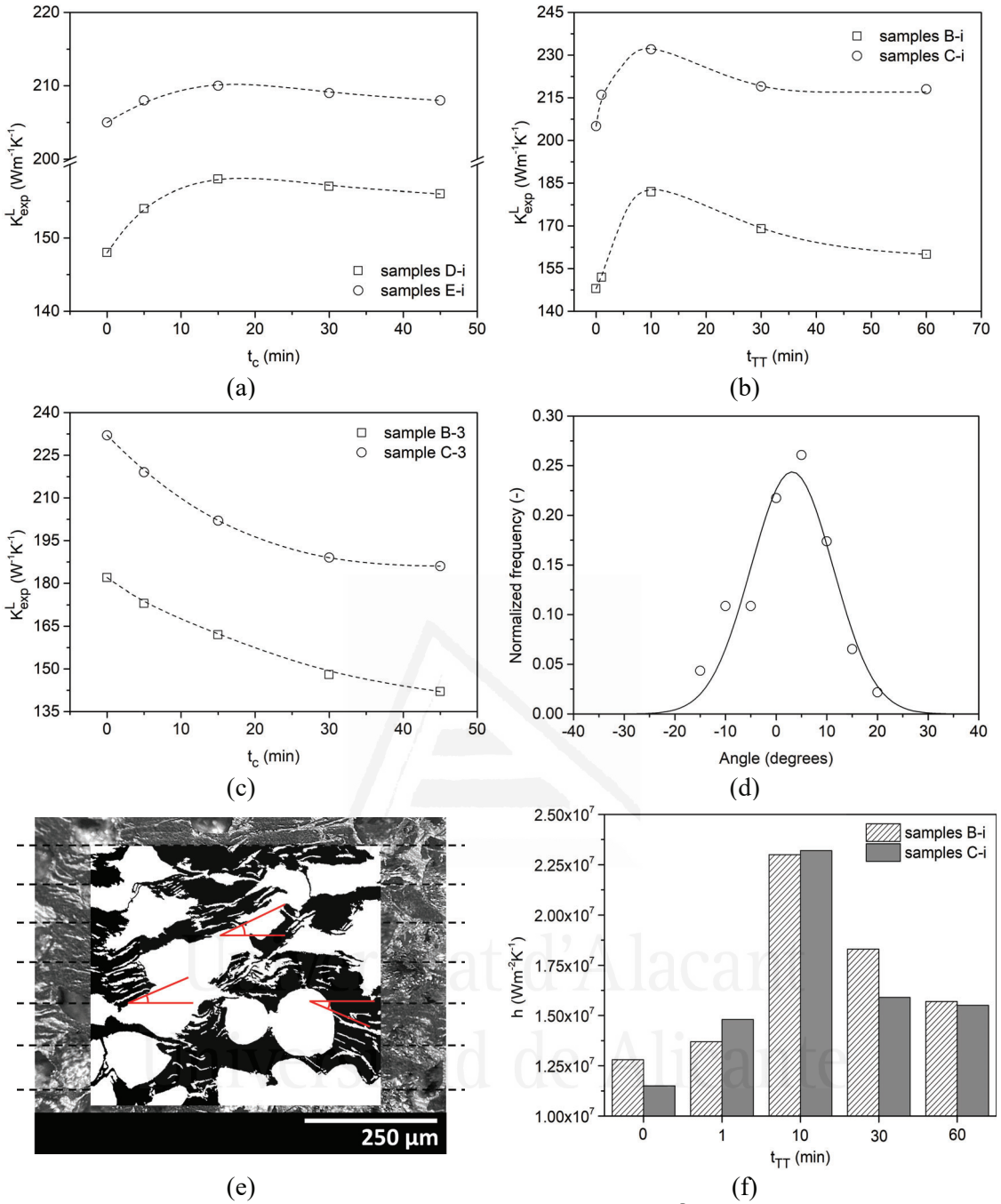

Figure 8. (a-c) Experimental longitudinal thermal conductivity (K^L_{exp}) versus: i) contact time (t_c) for samples with uncoated Gf – samples D-i and E-i (a), ii) coating treatment time (t_{TT}) for samples generated at t_c=0 –samples B-i and C-i (b), and iii) contact time (t_c) for samples with maximum thermal conductivity – samples B-3 and C-3 (c); (d) is the orientation distribution of Gf in sample B-3 derived from quantitative image analysis on polished and binarized images (see (e) for an illustration of binarization and orientation angle measurement with respect to ideal parallel lines); (f) is a bar diagram showing the interfacial thermal conductance of samples B-i and C-i derived from Equation (10).

Optimising the contact time in the Al/graphite system results in a maximum increase in thermal conductivity of 18 (samples D-i) and 16 (samples E-i) percent for a contact time of 15 minutes. This rise is in the order of that reported for the Al/diamond system, bearing in mind that in the present case we are considering foams and not composites, with a solid fraction of only 0.53. The thermal conductivity of the composite foams as a function of coating treatment time is depicted in Figure 8b. The trend observed is similar to that reported for the Al/diamond system, indicating that the greatest thermal conductivity is found at a particular time (in this case, t_{TT}= 10 min for both sets of samples with SiC-coated Gf). The infiltrations that resulted in the values shown in Figure 8b took place at nominal zero contact time. The thermal conductivity of these materials decreases with increasing contact time (Figure 8c), and the phenomenology associated with the underlying processes can be quite complex. While the main reaction between bare graphite flakes and aluminium is the formation of aluminium carbide, the presence of SiC complicates the reactivity as the reaction with aluminium produces both aluminium carbide and silicon, the latter being incorporated into the metal composition. As previously demonstrated in [34–37], the resulting silicon is expected to dissolve in the metal after a specified contact time, decreasing its intrinsic thermal conductivity. On the basis of the above it can be deduced that the optimum processing conditions can be determined as t_{TT}= 10 min and t_c= 0 min.

Analytical models can be used to calculate the interfacial conductance of the developed interfaces from the experimental values of thermal conductivity. For this purpose, an idealization of the obtained microstructures must be postulated. Composite foams are ternary systems consisting of metal, pores and thermal inclusions. It has been demonstrated that multicomponent systems can be treated in successive analytical steps, each focusing on a two-component system. The graphite flakes and metal in the present three-component system can be understood in such a way that they form a pseudo-matrix into which pores are later incorporated. Therefore, the first step in the analytical calculation is to consider the following expressions derived for the thermal conductivities in the longitudinal (K^L_{pm}) and transverse (K^T_{pm}) arrangements in microstructures containing platelet-shaped inclusions with a certain degree of orientation and uniformly distributed in a matrix [38,39]:

$$K^L_{pm} = K_m \left[\frac{2 + Vf[\beta_L(1-S_L)(1+cos^2\theta) + \beta_T(1-S_T)(1-cos^2\theta)]}{2 - Vf[\beta_L S_L(1+cos^2\theta) + \beta_T S_T(1-cos^2\theta)]}\right] \quad (4)$$

$$K^T_{pm} = K_m \left[\frac{1 + Vf[\beta_L(1-S_L)(1-cos^2\theta) + \beta_T(1-S_T)cos^2\theta]}{1 - Vf[\beta_L S_L(1-cos^2\theta) + \beta_T S_T cos^2\theta]}\right] \quad (5)$$

being

$$\langle cos^2\theta \rangle = \frac{\int \rho(\theta)\, cos^2\theta\, sin\theta\, d\theta}{\int \rho(\theta)\, sin\theta\, d\theta} \quad (6)$$

$$\beta_i = \frac{K_{eff}^i - K_m}{K_m + S_i\left(K_{eff}^i - K_m\right)}, \qquad (i = L, T) \tag{7}$$

where Vf refers to the volume fraction of the inclusion (Gf) in the aluminium matrix and $\cos^2\theta$ denotes its degree of orientation. K^i_{eff} is the effective thermal conductivity of the inclusion and S_i is a factor that takes into account its geometry and can be calculated as follows.

$$S_i = \frac{\pi t}{4D} \tag{8}$$

where t and D are the thickness and diameter, respectively. For the present calculations, the average diameters of Gf were estimated to be 150 and 500 μm, with average thicknesses of 10 and 20 μm, respectively. The fraction Vf of graphite flakes in the aluminium matrix is given by

$$Vf = \frac{V'f}{V'm + V'f} \tag{9}$$

being V'm and V'f the matrix and inclusion volume fractions in the ternary material.
In turn, the effective thermal conductivities (K^L_{eff} and K^T_{eff}) of the inclusion are related with the interfacial thermal conductance (h) as follows:

$$K_{eff}^L = \frac{K_{in}^L}{\frac{2K_{in}^L}{hD} + 1} \tag{10}$$

$$K_{eff}^T = \frac{K_{in}^T}{\frac{2K_{in}^T}{ht} + 1} \tag{11}$$

where K^i_{in} denotes the intrinsic thermal conductivity of the inclusions, which was assumed to be 1000 $Wm^{-1}K^{-1}$ in the Gf basal plane and 38 $Wm^{-1}K^{-1}$ in the perpendicular plane [15,20,22].
In a second step of the analytical calculation, pores are incorporated into the aluminium-graphite pseudo-matrix by using the following expression derived from the Generalized Differential Effective Medium Scheme (GDEMS), which has proven useful for calculating the thermal conductivity of foams composed of a matrix and a specific pore volume fraction:

$$K_F^i = K_{pm}^i\,(1 - V'p)^n, \quad \textit{(i=L,T)} \tag{12}$$

where K^{i}_{F} and V'p are the thermal conductivity of the composite foam and the pore volume fraction in the ternary system, respectively. The n exponent is a parameter related to the geometry of pores which, for spherical pores, is n = 3/2.

Most of the literature on Al/Gf composites assumes $\cos^2\theta=1$, which greatly simplifies the preceding equations. However, the presence of NaCl particles, the use of pressure for preform compaction, and the flexibility of the graphite flakes cause them to bend around the NaCl particles in the foams of the present work. Figure 8d depicts the orientation distribution of the graphite flakes in a representative sample (sample B-3) derived from an image analysis study in which cross-sectional images of the graphite flake planes were binarized and their angle of inclination with respect to perfect longitudinal reference lines was calculated (Figure 8e). From the experimental results and Equation (6) it was determined that $\cos^2\theta = 0.94$.

Figure 8f shows the theoretical values for the interfacial thermal conductance in the longitudinal direction calculated using Equation (10) for samples B-i and C-i, where the values in both series of samples are comparable because the thermal conductance is not a function of inclusion size. The h-values of the composite foams with uncoated Gf with an average diameter of 150 and 500 μm were determined to be 1.3×10^7 and 1.2×10^7 $Wm^{-2}K^{-1}$, respectively. These values are somewhat low compared to those obtained experimentally for the Al/graphite system, which are around 4.5×10^7 $Wm^{-2}K^{-1}$ [16,20,22]. This could be related to the fact that the metal does not completely cover the graphite flakes located at the surface of the pores (a similar phenomenology was observed in foams formed by magnesium matrix and thermal reinforcement of diamond particles [39]). The results correlate well with the thermal conductivity values presented in Figure 8b, where the maximum h-value for sample series B-i and C-i was obtained with SiC-coated Gf treated at t_{TT}= 10 min.

3.5 Mechanical properties

Aside from their thermal properties, another major issue with these materials is their flexural modulus, since they are usually embedded in electronic modules via anchors that impose a certain bending stress. Figure 9 depicts the Young's modulus (E) of selected specimens as a function of coating treatment time for SiC-coating of Gf obtained in three-point bending tests and under the experimental conditions specified in Section 2.4.4. The data presented are the average of three individual measurements. Graphite flakes, which are excellent thermal inclusions, appear at first glance to be inefficient as mechanical reinforcements. The modulus values perpendicular to the x-z plane for samples A-l and A-2, the replicated conventional aluminium foams, were 5.5 and 5.6 GPa, respectively. These results are consistent with the expected trend from the literature for the measured Young's moduli for a wide range of replicated aluminium foams with porosity contents between 60% and 90% [40]. These authors investigated the effect of pore size (400 and

75 μm) and shape (spherical and angular) on the Young's modulus of the Al foams. They found that the mechanical properties of these materials changed significantly only when foams with the smallest spherical and angular pores were considered. Minor differences in A-1 and A-2 modulus values demonstrate, firstly, that the property is unaffected by the size of the pore structure. Moreover, it is confirmed that the pores in both samples, with average diameters of 105 and 315 μm, have a largely equivalent quasi-spherical morphology.

The presence of graphite flakes leads to a significant shift in the volume fractions of the phases present in the composite foams, as well as to a decrease in the metal volume fraction, and thus to a degradation of the mechanical properties. In [22], it was shown that increasing the proportion of graphite flakes in powder metallurgical Al/Gf composites decreases the mechanical properties of the material. The authors of [22] also showed that the flexural strength of Al/Gf composites increases by up to 95% when graphite flakes were coated with SiC. In this study, increases of more than 95 and 110 percent were observed when comparing the elastic modulus for sample series B-i and C-i, measured perpendicular to the x-z plane (Figure 9a). Materials with smaller graphite flake inclusions exhibit improved mechanical properties in both directions of measurement. Like the thermal conductivity, the elastic moduli show optimal values for Al foams with coated Gf, which do not coincide with the minimum and maximum t_{TT}. The highest E values were found for samples B-3 and C-3, indicating that these materials are ideal candidates for active heat dissipation. The orientation of the graphite flakes with respect to the applied bending force is another crucial issue to consider. When the load was applied perpendicular to the x-z plane of the materials, the values of elastic moduli were 2-3 times higher than when the force was applied perpendicular to the x-y plane. This was also observed in [18,22], where the flexural strengths reported for Al/Gf composites varied up to 8 times when the two configurations were compared.

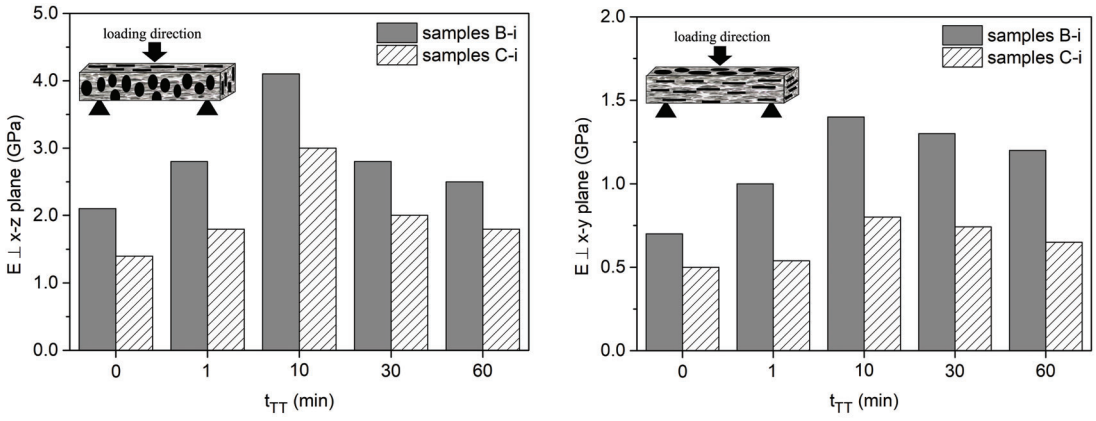

(a) (b)

Figure 9. Young´s modulus (E) of samples in perpendicular to the x-z (a) and x-y (b) plane, obtained from three-point bending tests.

3.6 Power dissipation

The thermal efficiency of a material when used as a heat sink is related to its high heat dissipation value and its low-pressure drop [7]. The material fabricated from large Gf particles with engineered SiC interfaces at t_{TT}= 10 min (sample C-3) proves to be the strongest competitor for thermal control applications among the composite foams fabricated and reported in this study. This material exhibits the highest thermal conductivity and permeability of all the materials fabricated, with a Young's modulus of 3 GPa, a value 27 percent lower than that of the analogous material fabricated with smaller graphite flakes and pores (sample B-3), but sufficient to meet application requirements. The power dissipation (P) of this sample, as well as that of other materials used for comparison, was measured using the equipment described in Section 2.4.3. To investigate the effects of the anisotropy of the materials, three different configurations of orientation with respect to the air inlet and heat source were employed, as shown in Figure 10a.

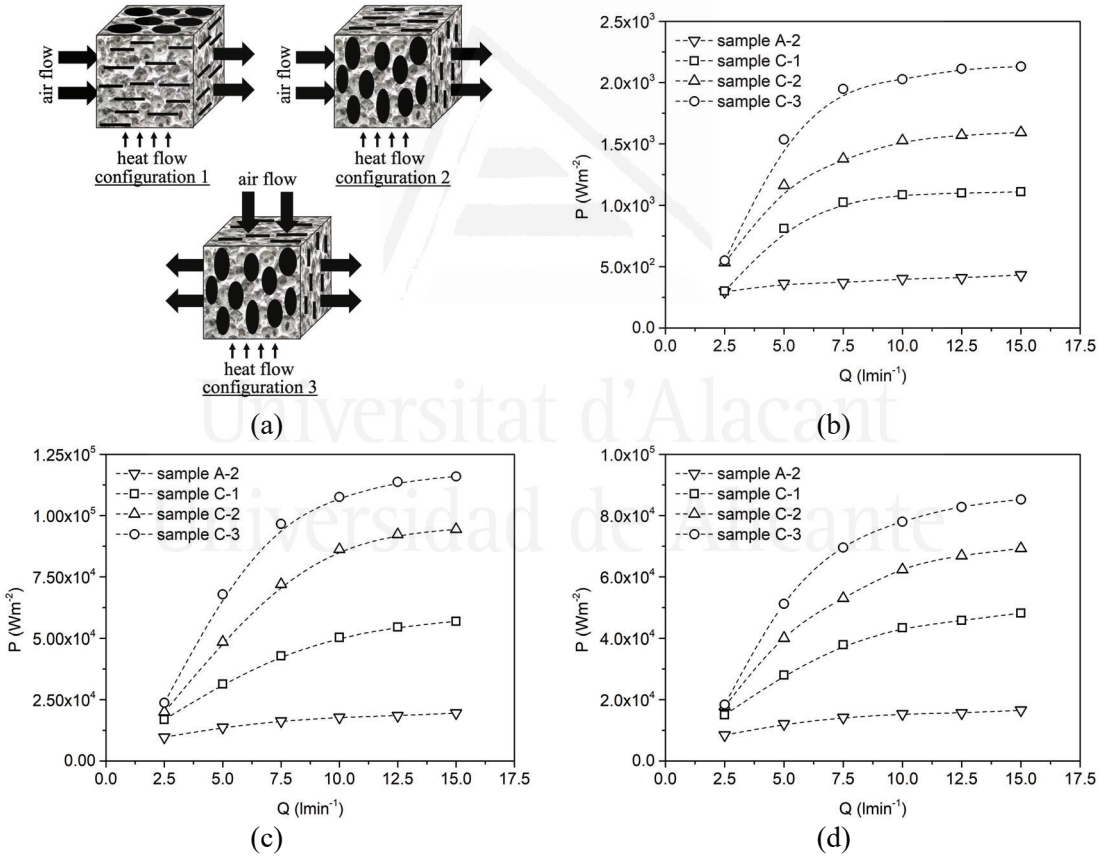

Figure 10. (a) Configurations employed for power dissipation experimental measurements. (b-d) are plots of P vs the volumetric air flow (Q) for samples A-2, C-1, C-2 and C-3.

Figure 10 shows that coating Gf with SiC significantly increases foam power dissipation in all configurations evaluated, which is consistent with the thermal conductivity values reported for each sample (compare samples C-1 with C-2 and C-3). Due to the perpendicular orientation of the graphite flakes with respect to the heat flux, the lowest P values were obtained in configuration

1 (see Figure 10b). Configuration 2, on the other hand, exhibited the highest power dissipation (Figure 10c). This is most likely due to the fact that the Gf are parallel to the heat flow (an orientation with higher thermal conductivity) and act as thermal guides, conducting heat to different parts of the material where it is evacuated by forced convection. In configuration 3 (Figure 10d), the material is arranged similarly to configuration 2, except that the air inlet is perpendicular to the heat source surface, resulting in two outlet surfaces. The P values in this configuration are slightly lower than in configuration 2 because the fluid is not channeled along the entire length of the material, but is ejected before fully passing through it, leaving regions of the material without an effective solid-fluid heat exchange by forced convection (these results are consistent with those in [10]).

When a volumetric air flow rate (Q) of 15 $lmin^{-1}$ is driven through the material in configuration 2, the power dissipation value of sample C-3 was 493% and 104% higher than those of the standard Al foam (sample A-2) and the material with uncoated Gf (sample C-1), respectively. As expected, sample C-3, which has the highest thermal conductivity, is the most efficient at dissipating heat through a conduction-convection mechanism.

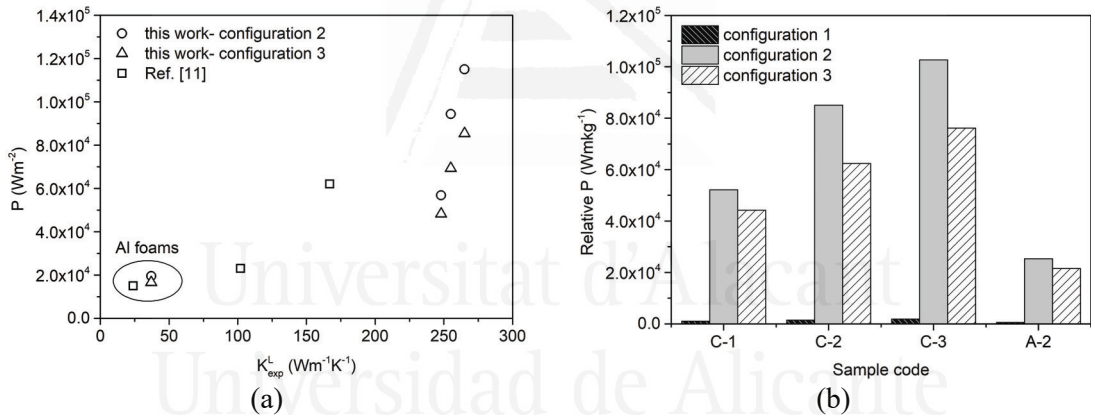

Figure 11. (a) Property map depicting the relationship between power dissipation (P) and thermal conductivity for various materials; (b) relative power dissipation for the various materials fabricated in this work.

The results in Figure 10 point out a direct relationship between the thermal conductivity of the different materials and the amount of heat they can dissipate. This relationship is illustrated in Figure 11a, which includes materials from the literature that have a comparable structure with oriented and uncoated Gf, as well as other standard Al foams, in addition to the materials fabricated in this work. It should be emphasized that in the vast majority of heat dissipation applications, weight is a first-order reject criterion. Apart from their utility as thermal inclusions, Gf have the added advantage of being exceptionally low dense. Figure 11b depicts the relative power dissipation (P divided by density) for the various materials produced in this work. The addition of Gf significantly improves the relative performance of conventional Al foam.

Moreover, the development of SiC-coated engineered interfaces improves heat dissipation performance, making these materials an extremely interesting target for future generations of electronic heat sinks.

4. Conclusions

The following conclusions can be drawn from the experimental evidence presented in this work:

- The replication method is sufficiently versatile to enable the fabrication of aluminium foams with thermal inclusions of oriented graphite flakes and an aluminium-graphite interface created by the incorporation of SiC.
- SiC incorporation at the aluminium-graphite interface was achieved by a molten salt synthesis method to coat the graphite flakes. Different coating degrees were obtained by varying the treatment time from 1 to 60 minutes.
- The effects of pore and graphite flake sizes on the fluid-dynamic and thermal performance of the materials were evaluated. The results indicate that foams with large pores derived from the use of large average sizes of NaCl templating agent have the advantage of generating low pressure drops. The best thermal conductivity was found for the foam that contained large graphite flakes that were coated during a 10-minute treatment. This material provided a thermal conductivity of 232 $Wm^{-1}K^{-1}$, a value 6 times higher than that of conventional replicated aluminium foams.
- Mechanical characterisation of the composite foams containing large graphite flakes reveals that the best thermal interface produced by a 10-minute SiC coating also exhibits the best mechanical behaviour, with a modulus of elasticity more than twice that of an unmodified interface. However, the mechanical properties of these foams are lower than those of conventional aluminum foams. This demonstrates that while graphite flakes are great thermal inclusions, they are poor mechanical reinforcements.
- It was found that the heat power dissipation of the optimised material is almost 500% greater than that of conventional aluminum foams or 104% higher than that of aluminium/graphite composite foams with unmodified interfaces, suggesting that this composite foam can be considered a serious candidate for future generations of heat sinks in electronics.

5. References

[1] Banhart J. Manufacture , characterisation and application of cellular metals and metal foams. Prog Mater Sci 2001;46:559–632.

[2] García-Moreno F. Commercial Applications of Metal Foams: Their Properties and Production. Materials (Basel) 2016;9:2–27. https://doi.org/10.3390/ma9020085.

[3] Zhao CY. Review on thermal transport in high porosity cellular metal foams with open

cells. Int J Heat Mass Transf 2012;55:3618–32. https://doi.org/10.1016/j.ijheatmasstransfer.2012.03.017.

[4] Zaragoza BG, Goodall R. Metal Foams with Graded Pore Size for Heat Transfer Applications. Adv Eng Mater 2012:1–6. https://doi.org/10.1002/adem.201200166.

[5] Bhattacharya A, Calmidi V V, Mahajan RL. Thermophysical properties of high porosity metal foams. Int J Heat Mass Transf 2002;45.

[6] Baloyo JM. Open-cell porous metals for thermal management applications: fluid flow and heat transfer. Mater Sci Technol 2016;33:265–76. https://doi.org/10.1080/02670836.2016.1180795.

[7] Hamadouche A, Nebbali R, Benahmed H, Kouidri A, Bousri A. Experimental investigation of convective heat transfer in an open-cell aluminum foams. Exp Therm Fluid Sci 2016;71:86–94. https://doi.org/10.1016/j.expthermflusci.2015.10.009.

[8] Mancin S, Zilio C, Diani A, Rossetto L. Air forced convection through metal foams : Experimental results and modeling. Int J Heat Mass Transf 2013;62:112–23. https://doi.org/10.1016/j.ijheatmasstransfer.2013.02.050.

[9] Maiorano Lauría LP, Molina-Jordá JM. Open-Pore Foams Modified by Incorporation of New Phases: Multiphase Foams for Thermal, Catalytic and Medical Emerging Applications. Foam. Emerg. Technol., IntechOpen; 2019. https://doi.org/10.5772/intechopen.88977.

[10] Maiorano LP, Molina JM. Guiding heat in active thermal management : One-pot incorporation of interfacial nano-engineered aluminium/diamond composites into aluminium foams. Compos Part A Appl Sci Manuf 2020;133:105859. https://doi.org/10.1016/j.compositesa.2020.105859.

[11] Maiorano LP, Molina JM. Challenging thermal management by incorporation of graphite into aluminium foams. Mater Des 2018;158:160–70. https://doi.org/10.1016/j.matdes.2018.08.026.

[12] Prieto R, Molina JM, Narciso J, Louis E. Thermal conductivity of graphite flakes – SiC particles metal composites. Compos Part A Appl Sci Manuf 2011;42:1970–7. https://doi.org/10.1016/j.compositesa.2011.08.022.

[13] Li W, Liu Y, Wu G. Preparation of graphite flakes/Al with preferred orientation and high thermal conductivity by squeeze casting. Carbon N Y 2015;95:545–51. https://doi.org/10.1016/j.carbon.2015.08.063.

[14] Zhou C, Ji G, Chen Z, Wang M, Addad A, Schryvers D, et al. Fabrication , interface characterization and modeling of oriented graphite flakes/Si/Al composites for thermal management applications. Mater Des 2014;63:719–28. https://doi.org/10.1016/j.matdes.2014.07.009.

[15] Xue C, Bai H, Tao PF, Jiang N, Wang SL. Analysis on Thermal Conductivity of

Graphite/Al Composite by Experimental and Modeling Study. J Mater Eng Perform 2017;26:327–34. https://doi.org/10.1007/s11665-016-2447-z.

[16] Li D, Wang C, Su Y, Zhang D, Ouyang Q. Governing the Inclination Angle of Graphite Flakes in the Graphite Flake/Al Composites by Controlling the Al Particle Size via Flake Powder Metallurgy. Acta Metall Sin (English Lett 2020;33:649–58. https://doi.org/10.1007/s40195-019-00994-0.

[17] Kurita H, Miyazaki T, Kawasaki A, Lu Y, Silvain J. Interfacial microstructure of graphite flake reinforced aluminum matrix composites fabricated via hot pressing. Compos Part A Appl Sci Manuf 2015;73:125–31. https://doi.org/10.1016/j.compositesa.2015.03.013.

[18] Li T, Liu ZY, Zan YN, Liu XY, Wang WG, Wang D, et al. Effect of nanometer SiC coating on thermal conductivity and bending strength of graphite flake/6063Al composites. J Alloys Compd 2021;862:3–9. https://doi.org/10.1016/j.jallcom.2020.158023.

[19] Shen Z, Ji G, Silvain J. From 1D to 2D arrangements of graphite flakes in an aluminium matrix composite : Impact on thermal properties. Scr Mater 2020;183:86–90. https://doi.org/10.1016/j.scriptamat.2020.03.022.

[20] Wang C, Bai H, Xue C, Tong X, Zhu Y, Jiang N. On the in fluence of carbide coating on the thermal conductivity and flexural strength of X (X=SiC, TiC) coated graphite/Al composites. R Soc Chem 2016;6:107483–90. https://doi.org/10.1039/c6ra21754k.

[21] N. Eustathopoulos, M.G. Nicholas BD. Wettability at High Temperatures. Amsterdam: Pergamon; 1999.

[22] Xue C, Bai H, Tao PF, Wang JW, Jiang N, Wang SL. Thermal conductivity and mechanical properties of flake graphite/Al composite with a SiC nano-layer on graphite surface. Mater Des 2016;108:250–8. https://doi.org/10.1016/j.matdes.2016.06.122.

[23] Han X, Huang Y, Ding L, Gao X, Xu Z. High thermal conductivity of GF@Cu@ Ni/Si/Al composites reinforced with Cu and Ni co-deposited graphite flakes. Ceram Int 2020;46:19191–7. https://doi.org/10.1016/j.ceramint.2020.04.254.

[24] Han X, Huang Y, Gao Q, Yu M, Chen X. High Thermal Conductivity and Mechanical Properties of Nanotube@Cu/ Ag@Graphite/Aluminum Composites. Ind Eng Chem Res 2018;57:10365–71. https://doi.org/10.1021/acs.iecr.8b01567.

[25] Chen J, Ren S, He X, Qu X. Properties and microstructure of nickel-coated graphite flakes/copper composites fabricated by spark plasma sintering. Carbon N Y 2017;121:25–34. https://doi.org/10.1016/j.carbon.2017.05.082.

[26] Masoudifar S, Bavand-vandchali M, Golestani-fard F, Nemati A. Molten salt synthesis of a SiC coating on graphite flakes for application in refractory castables. Ceram Int 2016;42:11951–7. https://doi.org/10.1016/j.ceramint.2016.04.120.

[27] Liu X, Zhang S. Low-Temperature Preparation of Titanium Carbide Coatings on Graphite Flakes from Molten Salts. J Am Ceram Soc 2008;91:667–70. https://doi.org/10.1111/j.1551-2916.2007.02184.x.

[28] Behboudi F, Kakroudi MG, Vafa NP, Faraji M, Milani SS. Molten salt synthesis of in-situ TiC coating on graphite flakes. Ceram Int 2021;47:8161–8. https://doi.org/10.1016/j.ceramint.2020.11.172.

[29] Conde Y, Despois JF, Goodall R, Marmottant A, Salvo L, Marchi CS, et al. Replication processing of highly porous materials. Adv Eng Mater 2006;8:795–803. https://doi.org/10.1002/adem.200600077.

[30] Molina-Jordá JM. Multi-scale design of novel materials for emerging challenges in active thermal management : Open-pore magnesium-diamond composite foams with nano-engineered interfaces. Compos Part A Appl Sci Manuf 2018;105:265–73. https://doi.org/10.1016/j.compositesa.2017.11.020.

[31] Otaru AJ. Review on Processing and Fluid Transport in Porous Metals with a Focus on Bottleneck Structures. Met Mater Int 2020;26:510–25. https://doi.org/10.1007/s12540-019-00345-9.

[32] Furman E, Finkelstein A, Cherny M. Permeability of Aluminium Foams Produced by Replication Casting. Metals (Basel) 2013:49–57. https://doi.org/10.3390/met3010049.

[33] Monje IE, Louis E, Molina JM. Optimizing thermal conductivity in gas-pressure infiltrated aluminum/diamond composites by precise processing control. Compos Part A Appl Sci Manuf 2013;48:9–14. https://doi.org/10.1016/j.compositesa.2012.12.010.

[34] Weber L, Sinicco G, Molina JM. Influence of processing route on electrical and thermal conductivity of Al/SiC composites with bimodal particle distribution. J Mater Sci 2010;45:2203–9. https://doi.org/10.1007/s10853-009-4060-0.

[35] Molina JM, Rhême M, Carron J, Weber L. Thermal conductivity of aluminum matrix composites reinforced with mixtures of diamond and SiC particles. Scr Mater 2008;58:393–6. https://doi.org/10.1016/j.scriptamat.2007.10.020.

[36] Molina JM, Narciso J, Weber L, Mortensen A, Louis E. Thermal conductivity of Al–SiC composites with monomodal and bimodal particle size distribution. Mater Sci Eng A 2008;480:483–8. https://doi.org/10.1016/j.msea.2007.07.026.

[37] Molina-Jordá JM. Design of composites for thermal management : Aluminum reinforced with diamond-containing bimodal particle mixtures. Compos Part A Appl Sci Manuf 2015;70:45–51. https://doi.org/10.1016/j.compositesa.2014.12.006.

[38] Chamroune N, Mereib D, Delange F, Caillault N, Lu Y, Grosseau-Poussard J-L, et al. Effect of flake powder metallurgy on thermal conductivity of graphite flakes reinforced aluminum matrix composites. J Mater Sci 2018;53:8180–92. https://doi.org/10.1007/s10853-018-2139-1.

[39] Nan C, Birringer R, Clarke DR, Gleiter H. Effective thermal conductivity of particulate composites with interfacial thermal resistance. J Appl Phys 1997;82:6692–9. https://doi.org/10.1063/1.365209.

[40] Goodall R, Marmottant A, Salvo L, Mortensen A. Spherical pore replicated microcellular aluminium : Processing and influence on properties. Mater Sci Eng A 2007;465:124–35. https://doi.org/10.1016/j.msea.2007.02.002.

Conclusions

Based on the developments conducted during the present PhD Thesis, the following conclusions are drawn:

- Conventional open-pore metal foams, whose thermal performance is insufficient to meet the thermal dissipation requirements of the most advanced electronic devices, have been redesigned by incorporating new phases (thermal inclusions).

- Metal foams could be produced with the desired microstructures by the well-known replication method. For this purpose, porous preforms consisting of compacts of a template agent (sodium chloride) and graphite flakes or diamond particles conveniently distributed, were prepared. By gas pressure infiltration of the preforms with liquid aluminium and subsequent removal of the template agent, four families of materials were obtained, differing in the nature of the thermal inclusion, in the distribution of the thermal inclusion in the matrix phase or in the metal-inclusion interface: i) aluminium foams with oriented graphite flakes homogeneously distributed in the matrix, ii) materials consisting of alternating layers of aluminium foam and oriented graphite flakes, iii) materials consisting of alternating layers of aluminium foam and aluminium/diamond composite material and iv) aluminium foams with oriented SiC-coated graphite flakes homogeneously distributed in the matrix.

- Aluminium foams incorporating graphite flakes exhibit longitudinal thermal conductivities in the range of 60-290 $Wm^{-1}K^{-1}$, with power dissipations up to 325% higher than that of conventional aluminium foams produced by the replication method. Moreover, the longitudinal thermal conductivities of foams incorporating diamond particles is in the range of 137-435 $Wm^{-1}K^{-1}$. These values can be significantly varied by the processing conditions, allowing a nano-dimensional control of the reaction products at the aluminium-diamond interface. The results reveal that the low thermal resistance interface between the aluminium foam and aluminium/diamond composite layers, derived from the one-pot infiltration synthesis, allows these materials to improve the thermal dissipation of the aluminium foams up to 130%. In this way, the composite layers act as thermal guides that transfer heat to the aluminium foam, where dissipation occurs by forced convection. It is also possible to modify the interface of aluminium foams incorporating graphite flakes by pre-coating them with SiC. The resulting thermal conductivity values can be adjusted by controlling the degree of graphite flakes coating, giving for an optimum interface a value of 232 $Wm^{-1}K^{-1}$ in a longitudinal arrangement and a power dissipation up to 500% higher than that of aluminium foams.

- Thermal conductivities of composite foams were successfully estimated using various analytical approaches that consider the microstructure of each material. A model was also used to verify experimental permeability values of foams incorporating graphite flakes, while computational modelling was employed to validate the experimental power dissipation results of aluminium/diamond multicomponent materials.

- Overall, the manufactured composite foams exhibit excellent thermal, fluid-dynamic and mechanical properties to be considered as suitable candidates for the most demanding thermal management applications in the electronics industry.

Conclusiones

De acuerdo con los desarrollos llevados a cabo durante la presente Tesis Doctoral, se exponen las siguientes conclusiones:

- Las espumas metálicas convencionales de poro abierto, cuyas prestaciones térmicas son insuficientes para cumplir con los requisitos de disipación térmica en los equipos electrónicos más avanzados, han sido rediseñadas mediante la incorporación de nuevas fases (inclusiones térmicas).

- Las espumas metálicas pudieron ser fabricadas con las microestructuras deseadas mediante el conocido método de replicación. Para ello, se prepararon preformas porosas que consistían en compactados de un agente plantilla (cloruro de sodio) y copos de grafito o partículas de diamante convenientemente distribuidas. Mediante la infiltración por presión de gas con aluminio líquido de las preformas y posterior eliminación del agente plantilla, se obtuvieron cuatro familias de materiales que difieren en la naturaleza de la inclusión térmica, en la distribución de la misma en la fase matriz o en la interfase metal-inclusión: i) espumas de aluminio con copos de grafito orientados y distribuidos homogéneamente en la matriz, ii) materiales formados por capas alternadas de espuma de aluminio y copos de grafito orientados, iii) materiales formados por capas alternadas de espuma de aluminio y material compuesto aluminio/diamante y iv) espumas de aluminio con copos de grafito orientados, recubiertos de SiC y distribuidos homogéneamente en la matriz.

- Las espumas de aluminio que incorporan copos de grafito presentan conductividades térmicas longitudinales dentro del intervalo de 60-290 $Wm^{-1}K^{-1}$, con potencias disipadas de hasta un 325% superior a las de las espumas de aluminio convencionales fabricadas por el método de replicación. Por otro lado, las conductividades térmicas longitudinales de las espumas que incorporan partículas de diamante se situa en el intervalo de 137-435 $Wm^{-1}K^{-1}$. Estos valores pueden variarse significativamente mediante las condiciones de procesado, lo que permite un control nanodimensional de los productos de reacción en la interfase aluminio-diamante. Los resultados revelan que la interfase de baja resistencia térmica entre las capas de espuma de aluminio y material compuesto aluminio/diamante, derivada de la síntesis por infiltración en un solo paso, permite que estos materiales mejoren hasta un 130% la disipación térmica de las espumas de aluminio. De este modo, las capas de material compuesto actúan como guías térmicas que transfieren el calor a la espuma de aluminio, donde la disipación se produce por convección forzada. Así mismo, es posible modificar la interfase de espumas de aluminio que incorporan copos de grafito, mediante el recubrimiento previo de los mismos con SiC. Los valores de conductividad

térmica resultantes pueden ajustarse controlando el grado de recubrimiento de los copos, obteniéndose para una interfase óptima un valor de 232 $Wm^{-1}K^{-1}$ en una disposición longitudinal y una potencia disipada de hasta un 500% superior a la de las espumas de aluminio.

- Las conductividades térmicas de las espumas de material compuesto fueron satisfactoriamente estimadas mediante diversas aproximaciones analíticas que contemplan la microestructura de cada material. Así mismo, se empleó un modelo para verificar los valores experimentales de permeabilidad en espumas que incorporan copos de grafito, mientras que la modelización computacional fue empleada para validar los resultados experimentales de potencia disipada en materiales multicomponente aluminio/diamante.

- En su conjunto, las espumas de material compuesto fabricadas presentan excelentes propiedades térmicas, fluidodinámicas y mecánicas para ser consideradas candidatas idóneas en las aplicaciones más exigentes de control térmico en la industria electrónica.

Future studies

The results derived from this PhD Thesis confirm the possibility of reformulating the designs of conventional metal foams, allowing their application as active heat sinks in emerging technologies. The incorporation of new phases into open-pore foams, however, is a strategy that remains open to further exploration.

Future studies suggest considering three interesting routes of action: i) the design of foams incorporating new phases with modified matrix-inclusion interfaces; ii) the design of foams incorporating a combination of new phases with modified interfaces; and iii) the design of foams incorporating new phases hosted in the porous cavities with no bound to the structural matrix (Guefoam-type foams). The following table collects some of the materials proposed to be developed in future studies.

Details of aluminium foams incorporating new phases proposed for future studies.

Material code	Matrix	Inclusion	Matrix-inclusion interface modification	Interest
Al/Gf_{TiC}	aluminium	graphite flakes (Gf)	pre-coating of Gf with TiC	-1-
Al/Gf_{SiC}-D		Gf and diamond particles (D)	pre-coating of Gf with SiC. Formation of Al_4C_3 at the Al-D interface during processing	-2- -3-
Al/Gf_{SiC}-D_{SiC}			pre-coating of Gf and D with SiC	-2- -3- -4-
Al/Gf_{SiC}-D_{TiC}			pre-coating of Gf with SiC and D with TiC	-2- -3- -4-
Al-[C or SiC]		carbon or SiC particles as guest phase	none or any of the above	-5-

-1- Aluminium/graphite flake composites with interfaces modified by pre-coating the reinforcements with TiC have shown superior mechanical properties to those with SiC-coated graphite flakes. Even though TiC provides a poor thermal interface, it is thought necessary to evaluate this system in aluminium foams for applications where mechanical properties are critical. Another factor to consider is the reduced density of these materials in comparison to the others presented in the table.

-2- The combination of graphite flakes and diamond particles can significantly increase the thermal conductivity and mechanical response of materials if the corresponding interfaces are properly controlled.

-3- The results obtained in Chapters 3 and 4 of this PhD Thesis demonstrated that the formation of aluminium carbide during processing is thermally favourable for the aluminium/diamond

system while unfavourable for the aluminium/graphite flakes system. For this purpose, it is suggested that the incorporated graphite flakes be pre-coated with SiC.

-4- Pre-coating the diamond particles with different metal carbides allows for comparison and optimisation of the different systems.

-5- The presence of guest phases in the cavities of aluminium foams can aid promote the convection mechanism, whereby heat is transferred from the structural solid matrix to a moving fluid (air). The main reason for this hypothesis is that the presence of new particulate phases, which are accommodated inside the pores and are not bound to the matrix, is likely to increase the degree of turbulence, which increases fluid-matrix interaction and allows for greater heat exchange between them.

The development of these materials is projected to be of great interest in the field of Materials Science, with a high scientific and technological impact.

Furthermore, the novelty of the systems presented in the preceding table implies an exhaustive characterisation of their thermal and fluid-dynamic behaviour. Since this characterisation can involve long execution times, the use of computational simulation tools is suggested for their optimisation. There are several programs designed for this purpose, being Ansys-Fluent one of the most widely used. This tool enables appropriate evaluation of the thermal properties (such as thermal conductivity and heat transfer coefficient) and fluid-dynamic properties (such as pressure drop and permeability) of the proposed materials, both at the pore scale and at the real scale. The software can also be used to evaluate certain design conditions, such as the orientation of heat sinks in electronic packaging (due to anisotropy of the materials manufactured) or the size of the heat sinks to achieve greater thermal efficiency. Thanks to the stay carried out by the PhD candidate, during which she performed computational thermal and fluid-dynamic simulations with an experienced group in the area (HTGroup), a multidisciplinary collaboration was generated which aims to open a research line of high scientific interest. This work, which is currently in progress, is based on the following hypothesis. The characteristic pore structure of a foam determines the fluid-dynamic and, consequently, the thermal behaviour of the material. The pore connecting windows generated by infiltration of martyr preforms are the areas of the foam material with the strongest restriction for the passage of a fluid. Therefore, it is considered necessary to evaluate the effect of the pore connecting window sizes on the properties of replicated open-pore foams. Preliminary computational results indicate that this design variable influence the thermal and fluid-dynamic parameters of the materials considered. While heat transfer coefficient and pressure drop relate inversely to the window size, the thermal efficiency is directly related to it.

Academic curriculum

The PhD candidate, Lucila Paola Maiorano Lauria, obtained her degree in Chemistry at the University of Alicante (UA) in 2016. She is currently a PhD student in Materials Science at the UA. In 2018 she was hired for a one-year period as part of a Ministry of Science and Innovation project, and in January 2020 she was awarded a three-year contract for pre-doctoral training supported by the "Vicerrectorado de Investigación" of the UA. At the end of 2021 she received a grant for short stays abroad, during which she worked at the University Luigi Vanvitelli (Italy) on thermal and fluid-dynamic computational simulations in metal foams.

Since the beginning of her career as a PhD student, she has published 6 scientific articles, 1 open access book chapter and 3 further articles are currently under review. She has contributed to 18 scientific conferences/meetings and is co-author of 3 business secrets. In the field of Educational Sciences, she has published 17 book chapters and contributed to 7 conferences.

Scientific publications in the field of Materials Science:

1. **L.P. Maiorano**, J.M. Molina. "Metal/Graphite flakes foams for heat sink applications". Asociación Española de Materiales Compuestos 2017; 2:35-41. (ISSN: 2531-0739)

2. G. Sarigul, **L.P. Maiorano**, J.M. Molina. "Development of carbon foams with hierarchical porosity". Asociación Española de Materiales Compuestos 2017; 2:30-34. (ISSN: 2531-0739)

3. **L.P. Maiorano**, J.M. Molina. "Challenging thermal management by incorporation of graphite into aluminium foams". Materials and Design 2018; 158:160-71. (DOI: 10.1016/j.matdes.2018.08.026)

4. **Lucila Paola Maiorano Lauria** and José Miguel Molina Jordá. "Open-Pore Foams Modified by Incorporation of New Phases: Multiphase Foams for Thermal, Catalytic and Medical Emerging Applications". Foams - Emerging Technologies, IntechOpen 2019. (DOI: 10.5772/intechopen.88977)

5. **L.P. Maiorano**, J.M. Molina. "Guiding heat in active termal management: One-pot incorporation of interfacial nano-engineered aluminium/diamond composites into aluminium foams". Composites Part A 2020; 133:105859. (DOI: 10.1016/j.compositesa.2020.105859)

6. J. Carbajo, **L.P. Maiorano**, J.M. Molina, N.X. Fang. "Sound absorption of macro-perforated additively manufactured media". Applied Acoustics 2021; 128:108204. (DOI: 10.1016/j.apacoust.2021.108204)

7. **L.P. Maiorano**, J.M. Molina. "Materiales multicomponente para disipación térmica con estructuras alternadas de espuma de Al y material compuesto Al/D". Asociación Española de Materiales Compuestos 2021; 5:67-72. (ISSN: 2531-0739)

8. F.C. Durmus, **L.P. Maiorano**, J.M. Molina. "Open-cell aluminum foams with bimodal pore size distributions for emerging thermal management applications". International Journal of Heat and Mass Transfer 2021. *Under review*.

9. **L.P. Maiorano**, C. Y. Chaparro-Garnica, E. Bailón García, D. Lozano-Castelló, A. Bueno-López, J.M. Molina-Jordá. "Guefoams (guest-containing foams) as novel

heterogeneous catalysts: preparation, characterization and proof-of-concept testing for CO_2 methanation" 2020. Materials and Design 2021. *Under review*.

10. **L.P. Maiorano**, R. Castillo, J.M. Molina. "Al/Gf composite foams with SiC-engineered interfaces for the next generation of active heat dissipation". Composites Part A 2022. *Under review*.

Developed objects of intellectual protection:

1. Business Secret entitled "Method of manufacturing spherical sodium chloride (NaCl) spherical shapes with an average diameter in the range 0.5 - 10 mm"
   Inventors: José Miguel Molina Jordá and **Lucila Paola Maiorano Lauria**.
   Holder: University of Alicante (Spain)
   Application number (date): 1310 (28/07/2020)

2. Business Secret entitled "Procedure for obtaining porous alumina (Al_2O_3) shapes with spherical geometry from finely divided particles"
   Inventors: José Miguel Molina Jordá and **Lucila Paola Maiorano Lauria**.
   Holder: University of Alicante (Spain)
   Application number (date): 1309 (28/07/2020)

3. Business Secret "Development of a method for the manufacture of spherical granules of solids from olive processing (alpechín)"
   Inventors: José Miguel Molina Jordá and **Lucila Paola Maiorano Lauria**.
   Holder: University of Alicante (Spain)
   Application number (date): 1308 (28/07/2020)

Publications in the field of Educational Sciences:

1. G. Casanova Pastor, T. Parra Santos, M.S. Sánchez Adsuar, M.J. Caturla Terol, E. Louis Cereceda, **L.P. Maiorano Lauria**, J.M. Molina Jordá. "INTERMAT VI (red de investigación INTERdisciplinar en MATeriales)". Memorias del Programa de Redes-I3CE de calidad, innovación e investigación en docencia universitaria. Convocatoria 2016-2017. Universidad de Alicante, Instituto de Ciencias de la Educación 2017; 1978-1981. (ISBN: 978-84-697-6536-4)

2. **L.P. Maiorano Lauria**, M.G. Derita, M. Martínez Escandell, J.M. Molina Jordá. "Estudio de las titulaciones "Profesorado en Química" y "Licenciado en Química" de la Universidad Nacional de Rosario (Argentina) para su adaptación al sistema universitario español". Redes-Innovaestic 2018. Libro de actas. Universidad de Alicante, Instituto de Ciencias de la Educación 2018; 67-68. (ISBN: 978-84-697-9429-6)

3. **L.P. Maiorano Lauria**, M.G. Derita, M. Martínez Escandell, J.M. Molina Jordá. "Estudio de las titulaciones "Profesorado en Química" y "Licenciado en Química" de la Universidad Nacional de Rosario (Argentina) para su adaptación al sistema universitario español". Redes de Investigación e Innovación en Docencia Universitaria. Volumen 2018. Universidad de Alicante, Instituto de Ciencias de la Educación 2018; 473-485. (ISBN: 978-84-697-9430-2)

4. **L.P Maiorano Lauria**, M.T. Parra Santos, J.A. Pons Botella, M.J. Caturla Terol, E. Louis Cereceda, M.S. Sánchez Adsuar, M. Martínez Escandell, J.M. Molina Jordá. "INTERMAT VII (red de investigación INTERdisciplinar en MATeriales)". Memorias del Programa de Redes-I3CE de calidad, innovación e investigación en docencia

universitaria. Convocatoria 2017-18. Universidad de Alicante, Instituto de Ciencias de la Educación 2018; 1031-1036. (ISBN: 978-84-09-07041-1)

5. G. Casanova Pastor, **L.P. Maiorano Lauria**, M. Teresa Parra Santos, J.M. Molina Jordá. "Chess game as pedagogical strategy for teaching: case study in Chemistry Degree". Proceedings of ICERI2018 Conference. IATED Digital Library 2018; 9596-9603. (ISBN: 978-84-09-05948-5)

6. G. Casanova Pastor, **L.P. Maiorano Lauria**, M. Teresa Parra Santos, J.M. Molina Jordá. "Study for qualifications in "Chemistry Teaching Degree" and "Chemistry Degree" from National University of Rosario-Argentina for its adaptation to the European system". Proceedings of ICERI2018 Conference. IATED Digital Library 2018; 9575-9583. (ISBN: 978-84-09-05948-5)

7. T. Parra Santos, J.M. Molina Jorda, G. Casanova Pastor, **L.P. Maiorano Lauria**. "Gamification for formative assessment in the framework of engineering learning". Proceedings of Sixth International Conference on Technological Ecosystems for Enhancing Multiculturality, TEEM'18. Association for Computing Machinery 2018; 61-65. (ISBN: 978-1-4503-6518-5)

8. **L.P. Maiorano Lauria**, M.T. Parra Santos, J.M. Molina Jordá. "Utilización de herramientas de gestión online para estudios de tercer ciclo en ciencias experimentales: universidad sin muros". Redes-Innovaestic 2019. Libro de actas. Universidad de Alicante, Instituto de Ciencias de la Educación 2019; 423. (ISBN: 978-84-09-07185-2)

9. **L.P Maiorano Lauria**, M.J. Caturla Terol, E. Louis Cereceda, M. Martínez Escandell, M.T. Parra Santos, J.A. Pons Botella, M.S. Sánchez Adsuar, J.M. Molina Jordá. "INTERMAT VIII (Red de investigación interdisciplinar en materiales)". Memorias del Programa de Redes-I3CE de calidad, innovación e investigación en docencia universitaria. Convocatoria 2018-19. Universidad de Alicante, Instituto de Ciencias de la Educación 2019; 2587-2604. (ISBN: 978-84-09-15746-4)

10. **L.P. Maiorano Lauria**, M.T. Parra Santos, J.M. Molina Jordá. "Universidad sin muros en estudios de ciencias experimentales de tercer ciclo: utilización de herramientas de gestión online". Redes de Investigación e Innovación en Docencia Universitaria. Volumen 2019. Universidad de Alicante, Instituto de Ciencias de la Educación 2019; 105-114. (ISBN: 978-84-09-07186-9)

11. T. Parra Santos, J.M. Molina Jordá, **L.P. Maiorano Lauria**, I. Milanovic, J.R. Pérez Domínguez. "Review Tasks of the Course's Contents". Seventh International Conference on Technological Ecosystems for Enhancing Multiculturality. Association for Computing Machinery 2019; 1-5. (ISBN 978-1-4503-7191-9/19/10)

12. C. Sabater Piqueres, **L.P. Maiorano Lauria**, M.T. Parra Santos, J.M. Molina Jordá. "Implementación de herramientas TIC interactivas e impresión 3D en el aprendizaje del enlace atómico". Redes-Innovaestic 2020. Libro de actas. Universidad de Alicante, Instituto de Ciencias de la Educación 2020; 474-475. (ISBN: 978-84-09-20651-3)

13. C. Sabater Piqueres, **L.P. Maiorano Lauria**, J.M. Molina Jordá. "Desarrollo y uso de herramientas TIC interactivas y modelos por impresión 3D en el aprendizaje a nivel universitario del enlace atómico". La docencia en la Enseñanza Superior. Nuevas aportaciones desde la investigación e innovación educativas. Octaedro 2020; 1333-1343. (ISBN: 978-84-18348-11-2)

14. **L.P Maiorano Lauria**, M.J. Caturla Terol, E. Louis Cereceda, M. Martínez Escandell, M.T. Parra Santos, J.A. Pons Botella, M.S. Sánchez Adsuar, C. Sabater Piqueres, J.M. Molina Jordá. "INTERMAT IX (RED DE INVESTIGACIÓN INTERDISCIPLINAR EN MATERIALES). Memorias del Programa de Redes-I3CE de calidad, innovación e investigación en docencia universitaria. Convocatoria 2019-20. Universidad de Alicante, Instituto de Ciencias de la Educación 2020; 585-592. (ISBN: 978-84-09-24478-2)

15. **L.P. Maiorano Lauria**, N. Verdú Molina, C. Sabater Piqueres, M.R. Calvo Urbina, J.M. Molina Jordá. "Integración en la enseñanza experimental de materiales compuestos desarrollados mediante herramientas de impresión 3D". Redes-Innovaestic 2021. Libro de actas. Universidad de Alicante, Instituto de Ciencias de la Educación 2021; 380-381. (ISBN: 978-84-09-29160-1)

16. **L.P. Maiorano Lauria**, N. Verdú Molina, C. Sabater Piqueres, M.R. Calvo Urbina, J.M. Molina Jordá. "Integración de herramientas de impresión 3D y simulación en la enseñanza experimental de los materiales compuestos". Nuevos retos educativos en la enseñanza superior frente al desafío COVID-19. Octaedro 2021; 339-350. (ISBN: 978-84-19023-19-3)

17. **L.P. Maiorano Lauria**, N. Verdú Molina, C. Sabater Piqueres, M.R. Calvo Urbina, C. Untiedt Lecuona, M.J. Caturla Terol, M. Martínez Escandell, J.A. Pons Botella, J. Silvestre Albero, J.M. Villalvilla Soria, J.M. Molina Jordá. "INTERMAT X (red de investigación INTERdisciplinar en MATeriales X). Universidad de Alicante, Instituto de Ciencias de la Educación 2021; 865-883. (ISBN: 978-84-09-34941-8)

Contributions to scientific congresses/meetings in the field of Materials Science:

1. Congress/meeting: XIII Jornadas Científicas de Instituto Universitario de Materiales
   Venue (date): University of Alicante, Spain (19-20/01/2017)
   Title: Metal/Graphite flakes foams for heat sink applications
   Type of communication: Poster
   Authors: **L.P. Maiorano**, J.M. Molina

2. Congress/meeting: XIII Jornadas Científicas de Instituto Universitario de Materiales
   Venue (date): University of Alicante, Spain (19-20/01/2017)
   Title: Development of carbon foams with hierarchical porosity
   Type of communication: Poster
   Authors: G. Sarigul, **L.P. Maiorano**, J.M. Molina

3. Congress/meeting: Foro Innova-T ADDA Alicante
   Venue (date): ADDA, Alicante, Spain (18-19/10/2017)
   Title: Grupo LMA-Laboratorio de Materiales Avanzados- de la Universidad de Alicante
   Type of communication: Oral-invited
   Authors: **L.P. Maiorano**, J.M. Molina

4. Congress/meeting: XII Congreso Nacional de Materiales Compuestos-MATCOMP17
   Venue (date): Palacio de Congresos Kursaal, San Sebastian, Spain (21-23/06/2017)
   Title: Espumas de metal/copos de grafito para aplicaciones de control térmico
   Type of communication: Oral
   Authors: **L.P. Maiorano**, J.M. Molina

5. Congress/meeting: XII Congreso Nacional de Materiales Compuestos-MATCOMP17
   Venue (date): Palacio de Congresos Kursaal, San Sebastian, Spain (21-23/06/2017)
   Title: Espumas de carbono con porosidad jerarquizada
   Type of communication: Poster
   Authors: G. Sarigul, **L.P. Maiorano**, J.M. Molina

6. Congress/meeting: XIV Jornadas Científicas de Instituto Universitario de Materiales
   Venue (date): University of Alicante, Alicante, Spain (18-19/01/2018)
   Title: Convective heat transfer properties of high thermal conductivity composite foams for active thermal management
   Type of communication: Poster
   Authors: **L.P. Maiorano**, J.M. Molina

7. Congress/meeting: XV Jornadas Científicas de Instituto Universitario de Materiales
   Venue (date): University of Alicante, Alicante, Spain (23-25/01/2019)
   Title: Challenging thermal management by incorporation of graphite into aluminium foams
   Type of communication: Poster
   Authors: **L.P. Maiorano**, J.M. Molina

8. Congress/meeting: XIII Congreso Nacional de Materiales Compuestos- MATCOMP19
   Venue (date): Sede Afundación, Vigo, Spain (3-5/07/2019)
   Title: Materiales multicomponente para disipación térmica con estructuras alternadas de espuma de aluminio y material compuesto aluminio/diamante
   Type of communication: Oral
   Authors: **L.P. Maiorano**, J.M. Molina

9. Congress/meeting: 9th International Conference on High Temperature Capillarity
   Venue (date): Budapest, Hungary-virtual (19-25/06/2020)
   Title: One-pot incorporation of interfacial nano-engineered Al/diamond composites into Al foams: new material designs for thermal management applications
   Type of communication: Poster
   Authors: **L.P. Maiorano**, J.M. Molina

10. Congress/meeting: 9th International Conference on High Temperature Capillarity
    Venue (date): Budapest, Hungary-virtual (19-25/06/2020)
    Title: Aluminium foams with graphite flakes fabricated by gas pressure infiltration technique for active thermal management
    Type of communication: Poster
    Authors: **L.P. Maiorano**, J.M. Molina

11. Congress/meeting: 9th International Conference on High Temperature Capillarity
    Venue (date): Budapest, Hungary-virtual (19-25/06/2020)
    Title: Thermal and fluid-dynamic behaviour of aluminium foams with bimodal pore size distribution
    Type of communication: Poster
    Authors: F.C. Durmus, **L.P. Maiorano**, J.M. Molina

12. Congress/meeting: XVI Jornadas Científicas de Instituto Universitario de Materiales
    Venue (date): University of Alicante, Alicante, Spain (23-24/01/2020)
    Title: Materiales multicomponente para disipación térmica con estructuras alternadas de espuma de Al y material compuesto Al/diamante
    Type of communication: Poster
    Authors: **L.P. Maiorano**, J.M. Molina

13. Congress/meeting: XVI Jornadas Científicas de Instituto Universitario de Materiales
    Venue (date): University of Alicante, Alicante, Spain (23-24/01/2020)
    Title: Materiales multifase basados en refuerzos bimodales de carbono contínuos-discontínuos para aplicaciones térmicas
    Type of communication: Poster
    Authors: M. Alfonso Gonzálvez, **L.P. Maiorano**, J.M. Molina

14. Congress/meeting: 6th International Conference on Nanoscience and Nanotechnology
    Venue (date): Kattankulathur, India-virtual (01-03/02/2021)
    Title: Optimizing the thermal performance of finned Al/diamond composite foams by incorporating nano-engineered interfaces
    Type of communication: Poster (BEST POSTER PRIZE, AWARDED BY SPRINGER NATURE)
    Authors: **L.P. Maiorano**, N. Verdú, J.M. Molina

15. Congress/meeting: XVII Jornadas Científicas de Instituto Universitario de Materiales
    Venue (date): University of Alicante, Alicante, Spain-virtual (03-04/06/2021)
    Title: Fabricación de espumas de Gf/C a partir de copos de grafito mediante una ruta de síntesis sencilla y económica
    Type of communication: Poster
    Authors: N. Verdú, **L.P. Maiorano**, J.M. Molina

16. Congress/meeting: XVII Jornadas Científicas de Instituto Universitario de Materiales
    Venue (date): University of Alicante, Alicante, Spain-virtual (03-04/06/2021)
    Title: Propiedades térmicas y mecánicas de espumas de Al que incorporan copos de grafito recubiertos de SiC
    Type of communication: Poster
    Authors: **L.P. Maiorano**, R. Castillo, J.M. Molina

17. Congress/meeting: XVII Jornadas Científicas de Instituto Universitario de Materiales
    Venue (date): University of Alicante, Alicante, Spain-virtual (03-04/06/2021)
    Title: Estudio de la corrosión de espumas de Mg con recubrimiento superficial para aplicaciones biomédicas
    Type of communication: Poster
    Authors: A. Nieto, **L.P. Maiorano**, J.M. Molina

18. Congress/meeting: European Congress and Exhibition on Advances Materials and Processes-EUROMAT-2021
    Venue (date): virtual (13-17/09/2021)
    Title: Simple and cost-effective fabrication of graphite/carbon foams from natural graphite flakes
    Type of communication: Poster
    Authors: N. Verdú, **L.P. Maiorano**, J.M. Molina

Contributions to scientific congresses/meetings in the field of Educational Sciences:

1. Congress/meeting: XVI Jornadas de Redes de Investigación en Docencia Universitaria, II workshop internacional de innovación en enseñanza superior y TiC- Redes Innovaestic 2018
    Venue (date): University of Alicante, Alicante, Spain (14-15/06/2018)
    Title: Estudio de las titulaciones "Profesorado en Química" y "Licenciado en Química" de la Universidad Nacional de Rosario (Argentina) para su adaptación al sistema universitario español
    Type of communication: Poster

Authors: **L.P. Maiorano**, M.G. Derita, M. Martínez Escandell, J.M. Molina

2. Congress/meeting: Sixth International Conference on Technological Ecosystems for Enhancing Multiculturality-TEEM'18
   Venue (date): University of Salamanca, Salamanca, Spain (24-26/10/2018)
   Title: Gamification for formative assessment in the framework of engineering learning
   Type of communication: Virtual
   Authors: M.T. Parra, J.M. Molina, G. Casanova, **L.P. Maiorano**

3. Congress/meeting: 11th annual International Conference of Education, Research and Innovation-ICERI2018
   Venue (date): Sevilla, Spain (12-14/11/2018)
   Title: Study for qualifications in "Chemistry Teaching Degree" and "Chemistry Degree" from National University of Rosario-Argentina for its adaptation to the European system
   Type of communication: Virtual
   Authors: **L.P. Maiorano**, M.G. Derita, M. Martínez Escandell, J.M. Molina

4. Congress/meeting: 11th annual International Conference of Education, Research and Innovation-ICERI2018
   Venue (date): Sevilla, Spain (12-14/11/2018)
   Type of communication: Virtual
   Title: Chess game as pedagogical strategy for teaching: case study in Chemistry Degree
   Authors: G. Casanova, **L.P. Maiorano**, M.T. Parra, J.M. Molina

5. Congress/meeting: XVII Jornadas de Redes de Investigación en Docencia Universitaria, III workshop internacional de innovación en enseñanza superior y TiC- Redes Innovaestic 2019
   Venue (date): University of Alicante, Alicante, Spain (06-07/06/2019)
   Type of communication: Poster
   Title: Utilización de herramientas de gestión online para estudios de tercer ciclo en ciencias experimentales: universidad sin muros
   Authors: **L.P. Maiorano**, M.T. Parra, J.M. Molina

6. Congress/meeting: XVIII Jornadas de Redes de Investigación en Docencia Universitaria, IV workshop internacional de innovación en enseñanza superior y TiC- Redes Innovaestic 2020
   Venue (date): University of Alicante, Alicante, Spain (04-11/06/2020)
   Type of communication: Oral
   Title: Implementación de herramientas TIC interactivas e impresión 3D en el aprendizaje del enlace atómico
   Authors: C. Sabater, **L.P. Maiorano**, J.M. Molina

7. Congress/meeting: XIX Jornadas de Redes de Investigación en Docencia Universitaria, V workshop internacional de innovación en enseñanza superior y TiC- Redes Innovaestic 2021
   Venue (date): University of Alicante, Alicante, Spain (10-16/06/2021)
   Type of communication: Oral
   Title: Integración en la enseñanza experimental de materiales compuestos desarrollados mediante herramientas de impresión 3D
   Authors: C. Sabater, N. Verdú, **L.P. Maiorano**, M.R. Calvo, J.M. Molina

Participation in science projects:

1. Project title: Desarrollo de materiales porosos 2D y 3D con aplicaciones electroquímicas, catalíticas, térmicas y biomédicas (MAT2016-77742-C2-2-P)
   Participation as: collaborator
   Responsible researcher: José Miguel Molina Jordá
   Number of participating researchers: 5
   Number of entities involved: 2
   Funding entity: Ministry of Science and Innovation
   Start date: 30/12/2016 end date: 20/09/2020
   Total amount: 50.000,00 €

2. Project title: Construcción, validación y acciones de transferencia de un prototipo de equipo portátil de purificación de aire para la eliminación de patógenos en ambientes cerrados (PDC2021-121617-C21)
   Participation as: collaborator
   Responsible researcher: José Miguel Molina Jordá
   Number of participating researchers: 5
   Number of entities involved: 1
   Funding entity: Ministry of Science and Innovation
   Start date: 01/12/2021 end date: 30/11/2023
   Total amount: 140.300,00 €

3. Project title: Desarrollo (fabricación y caracterización) de materiales espumados con fases huésped para purificación de aire por eliminación de virus y bacterias (GVA-COVID19/2021/100)
   Participation as: collaborator
   Responsible researcher: José Miguel Molina Jordá
   Number of participating researchers: 10
   Number of entities involved: 2
   Funding entity: Generalitat Valenciana
   Start date: 01/01/2022 end date: 31/12/2022
   Total amount: 70.418,75 €

4. Project title: Contratos destinados a la formación predoctoral (UAFPU2019-33)
   Participation as: coordinator
   Responsible researcher: **Lucila Paola Maiorano Lauria**
   Number of participating researchers: 1
   Number of entities involved: 1
   Funding entity: University of Alicante
   Start date: 16/01/2020 end date: 15/04/2023
   Total amount: 62.713,83 €

5. Project title: Estancia en Università degli Studi della Campania “Luigi Vanvitelli” (UAEEBB21-10)
   Participation as: coordinator
   Responsible researcher: **Lucila Paola Maiorano Lauria**
   Number of participating researchers: 1
   Number of entities involved: 1
   Funding entity: University of Alicante
   Start date: 15/09/2021 end date: 15/12/2021
   Total amount: 1.950,00 €

Participation in innovative teaching projects:

1. Project title: INTERMAT VI (red de investigación INTERdisciplinar de MATeriales)
   Redes I3-CE
   Participation as: member
   Responsible researcher: José Miguel Molina Jordá
   Number of participating researchers: 7
   Number of entities involved: 1
   Funding entity: University of Alicante
   Year: 2016-2017
   Total amount: 1.100,00 €

2. Project title: INTERMAT VII (red de investigación INTERdisciplinar de MATeriales)
   Redes I3CE
   Participation as: member
   Responsible researcher: José Miguel Molina Jordá
   Number of participating researchers: 8
   Number of entities involved: 1
   Funding entity: University of Alicante
   Year: 2017-2018
   Total amount: 1.500,00 €

3. Project title: INTERMAT VIII (red de investigación INTERdisciplinar de MATeriales)
   Redes I3CE
   Participation as: member
   Responsible researcher: José Miguel Molina Jordá
   Number of participating researchers: 8
   Number of entities involved: 1
   Funding entity: University of Alicante
   Year: 2018-2019
   Total amount: 1.500,00 €

4. Project title: INTERMAT IX (red de investigación INTERdisciplinar de MATeriales)
   Redes I3CE
   Participation as: member
   Responsible researcher: José Miguel Molina Jordá
   Number of participating researchers: 9
   Number of entities involved: 1
   Funding entity: University of Alicante
   Year: 2019-2020
   Total amount: 1.900,00 €

5. Project title: INTERMAT X (red de investigación INTERdisciplinar de MATeriales)
   Redes I3CE
   Participation as: member
   Responsible researcher: José Miguel Molina Jordá
   Number of participating researchers: 11
   Number of entities involved: 1
   Funding entity: University of Alicante
   Year: 2020-2021
   Total amount: 1.525,00 €

6. Project title: INTERMAT XI (red de investigación INTERdisciplinar de MATeriales)
   Redes I3CE
   Participation as: participant member
   Responsible researcher: José Miguel Molina Jordá
   Number of participating researchers: 11
   Number of entities involved: 1
   Funding entity: University of Alicante
   Year: 2021-2022
   Total amount: 2.401,00 €

Teaching activities:

1. Subject: Química del Estado Sólido (code: 35800)
   Department: Inorganic Chemistry
   Hours: 10
   Year: 2020-2021

2. Subject: Sólidos Inorgánicos (code: 26026)
   Department: Inorganic Chemistry
   Hours: 30
   Year: 2020-2021

3. Subject: Sólidos Inorgánicos (code: 26026)
   Department: Inorganic Chemistry
   Hours: 12
   Year: 2021-2022

4. Subject: Ciencia de Materiales (code: 26209)
   Department: Inorganic Chemistry
   Hours: 18
   Year: 2021-2022